CHALMERS

Investigation of Magnetic Resonance Imaging Effects when Using Bone Conduction Implants

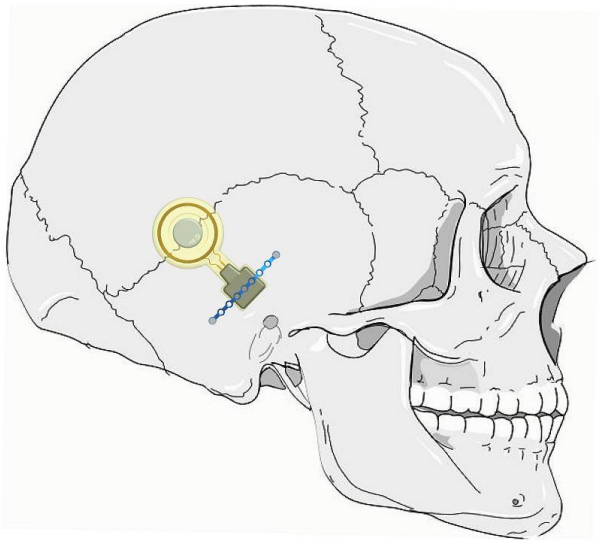

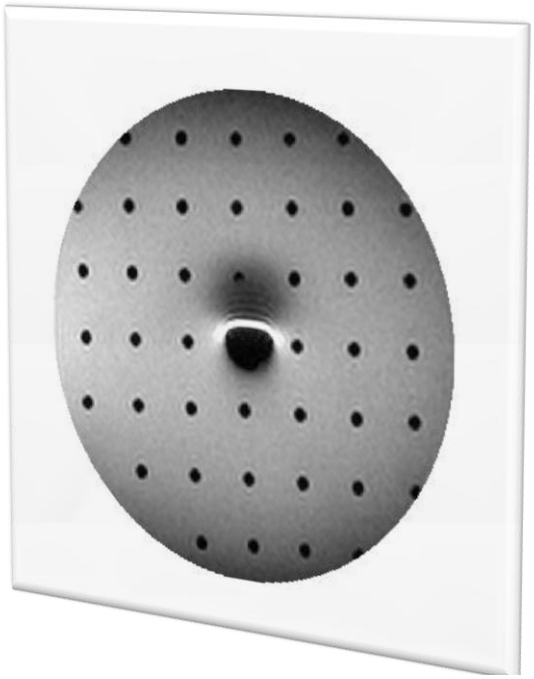

Master of Science Thesis in Biomedical Engineering, MPBME

Karl-Johan Fredén Jansson

Department of Signals and Systems

CHALMERS UNIVERSITY OF TECHNOLOGY

Göteborg, Sweden, 2011

Report No. EX042/2011

Abstract

The Bone Conduction Implant (BCI) is a new hearing implant for patients with conductive or mixed hearing loss or that can't use normal air conduction hearing aids for some reason. The BCI has an external and an internal part that are held in place by magnetic coupling through the skin. The external part picks up the sound and then transmits it electromagnetically to the internal part that converts it to mechanical vibrations by a transducer in the temporal bone. These vibrations are led to the cochlea where they will be perceived as sound.

Safety aspects for patients with the BCI that has to undergo Magnetic Resonance Imaging (MRI) have been investigated. Magnetic materials in the implant cause problems from interactions with the electromagnetic fields in the MRI scanner. Effects such as forces, vibrations, demagnetization, heat generation and image artifacts have been studied in simulations and by experiments. Simulations have been done in COMSOL Multiphysics and experiments have been done at the Sahlgrenska University Hospital. Image artifacts can be minimized by the choice of pulse sequence, but other problems need a modification of the implant.

The internal part is the only part of the BCI that is exposed to the MRI fields since the external part easily can be removed before doing a MRI examination. Both the holding magnet and magnets in the transducer will interact with magnetic fields in the scanner.

Force measurements have been done and images for different pulse sequences have been obtained for two types of magnets, Samarium-Cobalt (SmCo) and Neodymium-Iron-Bohr (NdFeB). NdFeB magnets are more easily demagnetized than SmCo and the demagnetization is strongly dependent on the angle between the magnet's magnetization direction and the direction of the static magnetic field of the scanner.

For the transducer an idea to use high permeability materials to shield its magnets from the electromagnetic fields has been evaluated with simulations and tested in a MRI scanner. Simulations show that it is theoretically possible to use this type of shielding. In the experiments new problems occurred such as vibrations of the transducer.

Acknowledgement

I want to thank Professor Bo Håkansson for giving me the opportunity to do this master thesis and for all his participation in meetings and experiments. Also thanks to my supervisor Sabine Reinfeldt for all the good support and feedback on my work and her participation in the project. At the department of signals and systems also thank Hamidreza Taghavi for particaipation at the experiments, Oscar Talcoth for helping me starting the project. At Sahlgrenska University Hospital thank to Åsa Carlsson, and Kerstin Lagerstrand for making the experiments possible and to all the good support. Also thank to Göran Stark for the lectures in magnetic resonance imaging. Thank to Magnus Haglund at SuraMagnets for supporting me with the magnets and measurements and also thank to Jacob Blomgren at Imego for all the Gaussmeter measurements.

Abbreviations

MRI – Magnetic Resonance Imaging

BAHA – Bone Anchored Hearing Aid

BCI – Bone Conduction Implant

CT – Computed Tomography

FMT – Floating Mass Transducer

EPI – Echo Planar Imaging

FFE – Fast Field Echo

T1W – T1 Weighted

SE – Spin Echo

GE – Gradient Echo

RF – Radio Frequency

Table of Contents

1 Introduction

Patients who are suffering from conductive or mixed hearing loss, or single sided deafness are sometimes poorly rehabilitated by conventional air conduction hearing aids (due to functionality losses in the middle or outer ear). In these hearing losses, the cochlea functions perfectly, and a bone conduction hearing aid is applied to transmit sound data more efficiently to the cochlea.
A full Bone Conduction Implant (BCI) system comprises two separated parts; the external unit which includes microphone, digital signal processor and transmitter coil with battery compartment. The implanted unit contains the receiver coil and the transducer, see Figure 1-1. The transducer converts the sound data to vibrations by a complicated electromagnetic-electromechanical technique (Håkansson, 2003). This part is implanted in the temporal bone in skull, see Figure 2-1.

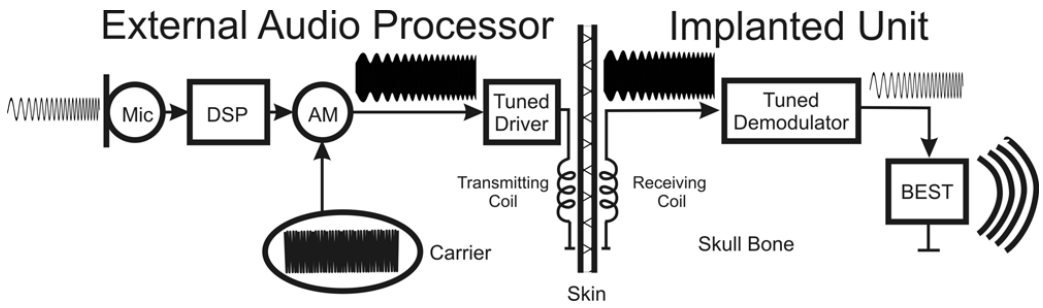

Figure 1-1: A detailed scheme of all the different steps over the BCI system from input signal to output signal. The external audio processor is seen to the left and the internal implanted unit is seen to the right. The signal is transmitted from the external to the internal part by a transmitting coil and a receiving coil respectively (Håkansson et al, 2010).

Magnetic Resonance Imaging (MRI) is getting more widely used as a tool for medical diagnoses since it has the advantage compared to other imaging techniques to distinguish between different tissues in the body. MRI is a non-ionizing radiation method that has not shown any signs of being harmful to the patient.

However a MRI examination is complicated for patients that have medical implants in their body. The implant has a potential risk of injuring the patient or damaging the implant because the strong electromagnetic fields of the scanner interact with the implant in an undesirable way. The effects of different magnetic fields such as the static magnetic field (B_0) field, the Radio Frequency (RF) field and the gradients are therefore needed to be investigated.

Before doing a MRI it has to be evaluated if it is possible to use another imaging technique e.g. Computed Tomography (CT), for the same survey. That might involve other risks or doesn't give a diagnosis that is good enough. To avoid surgically removal of the implant when a patient needs to do a MRI, the goal is to make the implant MRI-compatible by reducing the dangerous potential risks that it includes. This project focuses on making the BCI MRI-compatible. Research in this area has earlier been done for other hearing implants like the Cochlear Implant (CI), the Bone Anchored Hearing Aid (BAHA) and the Floating Mass Transducer (FMT). From this earlier research that has been going on for over 20 years (Teissl et al, 1998), several ideas can be used to find a solution for the BCI. One main thing that makes the BCI different from many other hearing devices in a MRI environment is the part that also makes it different in the sense of operating as a hearing device, namely the implanted Bone Conduction (BC) transducer. The design of the transducer consists of a special arrangement of magnets to achieve optimal transferring of sound vibrations to the cochlea. The BCI have magnets in both the holding housing part and the transducer that will interact with the field from a MRI scanner.

Compared to other hearing implants this has more magnets and the BCI will need a modification of both the holding magnet and the transducer magnets in order to make it MRI compatible. The magnetic parts of the implant can be affected in terms of forces, demagnetization, heat generation, and vibrations. First of all, it is the patient's safety that is important and forces, heat and vibrations might do harm to the patient. Secondly, the implant can easily lose all of its performance and function if the magnets of the transducer get demagnetized.

The aim of this project is to investigate the effects of MRI fields on the BCI by simulations using the software COMSOL Multiphysics and compare the results by experimental measurements performed at Sahlgrenska University Hospital Imaging Department.

2 Theory

2.1 The Bone Conduction Implant

The BCI consists of one external and one internal part, see Figure 2-1 .The external part has a holding magnet, an audio signal processor and a transmitter induction link. The internal part has a holding magnet, a receiver induction link and a transducer. The only thing that holds the internal and external part in place is permanent magnets. This makes it possible to remove the external part from the internal before doing a MRI examination. The internal part can only be removed by surgery. To avoid surgery, this part is necessary to consider when investigating the MRI effects on the BCI.

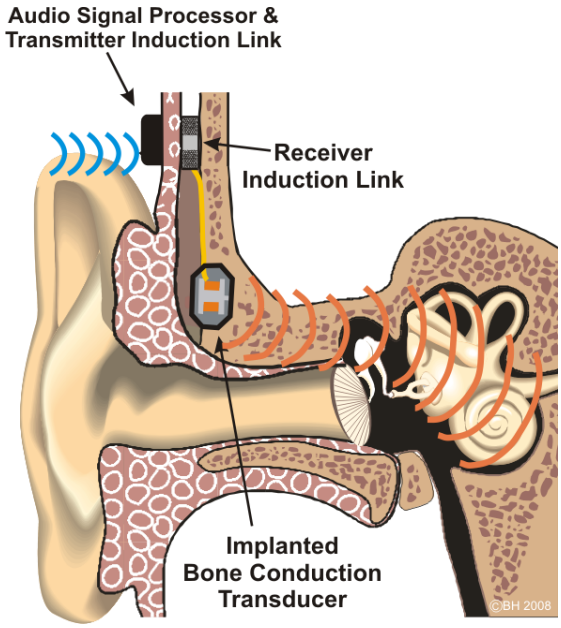

Figure 2-1: The different parts of the Bone Conduction Implant system. The transducer is connected to the receiver induction link and implanted in the temporal bone. The external transmitter induction link send signals from the audio signal processor to the receiver induction link by a transcutaneous wireless communication system (Håkansson el al, 2008).

2.2 Magnetic Resonance Imaging

Magnetic Resonance Imaging (MRI) is a clinical imaging method used to take images inside the human body. It's a non-ionizing and non-invasive method. To create the images, the MRI scanner uses a static magnetic field, radio frequency (RF) pulses and gradient fields applied to the body or the body part of interest. If this is done properly it will interact with the hydrogen nuclei in the body in such a way that a measureable signal will be emitted from the tissues consisting of hydrogen. This signal is then translated into a grayscale image that can be analyzed for diagnostics of the patient.

2.2.1 Static magnetic field

The static B-field is a strong external magnetic field from the MRI scanner which is usually between 1.5 Tesla (T) and 3T, but there also exists scanners with higher field strengths such as 7T and 9.4T scanners. The higher field strengths make it possible for diagnosis with other applications such as functional MRI where with the 9.4T scanner it is in the future believed to be possible to track the firing of neurons and thereby study how thoughts are formed (ELLIS D, 2007).

The static magnetic field is usually given in the unit Tesla (T) which is the unit of magnetic flux density not to confuse with the magnetic field that in electromagnetism is given in Ampere/meter (A/m).

When this field is applied to the body it aligns the magnetic moments of the hydrogen nuclei's in the tissues in the same direction as itself. This will result in that the tissues in the body will have a unique net magnetization that differs from the static magnetic field. This magnetization difference is big enough to be measurable and it is possible to interact with it by applying time-varying RF- and gradient-fields to it. By studying how it will respond to those fields it is possible to distinguish the different types of tissue in the body.

2.2.2 Spin

The net magnetization in the tissue from the alignment of the hydrogen nuclei's will have a so called nuclear magnetic moment. In solid state physics, electrons are said to have a mass, a charge and a spin which are properties that describes the nuclear magnetic moment. The spin during thermal equilibrium can for an electron be either 1/2 or -1/2. The net spin is the summation of all the spins in the tissue. If two spins are anti-parallel to each other the net spin of them will be zero. The spin direction is perpendicular to the magnetization and creates a magnetic dipole moment, which is the nuclear magnetic moment.

2.2.3 RF-pulse

The spins can be excited from their thermal equilibrium with an RF-pulse in such a way that the magnetic dipole moment will deviate from the direction or alignment of the static magnetic field. When the RF-pulse is turned off, the magnetic dipole moment will fall back to the direction of the static magnetic field in a gyrometric motion as the energy of the spin itself falls back to thermal equilibrium. To excite the spins with an RF-pulse its main frequency component is the so called Larmor frequency f_l, which depends on the static magnetic field and the gyrometric properties of hydrogen.

$$f_l = \gamma B_0 \tag{1}$$

where γ is the gyrometric constant for hydrogen nuclei and B_0 is the magnetic flux density of the static magnetic field. For hydrogen $\gamma = 42{,}58\ MHz/T$. The RF-pulse usually has an amplitude of 14μT (Shellock et al, 2005) with frequencies varying from 10-200MHz (C. Bushong, 2003). The RF signal is transmitted and received perpendicular to the direction of the static magnetic field by something called RF-coils. Sometimes the same RF-coil is used both as a transmitter and receiver. To get better accuracy, in some cases multiple number of RF-coils are used together. For example a head coil that is placed around the patient's head during brain imaging. Then the received RF-signal will be high only from the part of the body that is inside this coil and low from the rest of the body. This will reduce noise and artifacts that comes from other body parts (C. Bushong, 2003).

2.2.4 Gradient Fields

The RF-pulse is sent together with something that is called a gradient field. This allows the pulse to be focused on a specific point and create slices over the area of interest for different amplitude and phase. The gradient fields linearly change the direction of the static magnetic field in three dimensions. When the gradient is applied, it means that the magnetic flux density is different for every scanning point and thereby also the Larmor frequency. This makes it possible to choose from where to get the received RF signal back. The gradient field usually has maximum amplitude of 40mT/m.

2.2.5 Pulse sequences

There are different kinds of sequences that the RF-pulse and gradient fields can be sent in to interact with the magnetic dipole moment differently in order to create the T1 and T2 images. The most common sequences to create slices are Gradient Echo (GE) and Spin Echo (SE). The SE sequence is more insensitive to magnetic susceptibility artifacts, which makes the SE sequence more suitable for imaging medically implanted devices. What characterizes the SE sequence is that that it includes one 90 and one 180 degree pulse compared to the GE sequence that only consists of one 90 degree pulse.

2.2.6 T1 & T2 images

The measured signal from the relaxation of the magnetic dipole moment relaxation has a longitudinal and transversal component which is translated into two grayscale images. The image taken from the longitudinal component is called the T1 image, which is a grayscale image computed from the spin-lattice relaxation times. The transversal component will give an image that is called the T2 image, which is created out of the spin-spin relaxation times.

2.2.7 Clinical views

In MRI brain imaging, there are usually three different views from which the reconstructed image is analyzed from and these are sagittal, coronal and collateral. Three dimensional images are also used, but not always necessary and time consuming.

2.2.8 MRI and medical implants

There are different types of magnetic materials. They're distinguished by their magnetic properties. If magnetic materials are implanted in the body during a MRI examination, they can interact in different ways with the magnetic field from the scanner. This can for example lead to forces on the material, heating of it and have effects on the image in the area of the implant. The nuclear magnetic moments in the body are aligned in the direction of the static B-field because they act like small magnets.

2.3 MRI effects on the BCI

2.3.1 Maxwell's Equations

The effect of time-varying electromagnetic fields in the MRI scanner, such as induced currents and voltages in conductive loops, can be described by Maxwell's equations. For MRI applications Faraday's law can be used to relate the electrical field $\vec{E}$ with the magnetic flux density $\vec{B}$:

$$\nabla \times \vec{E} = -\frac{\partial \vec{B}}{\partial t} \tag{2}$$

This can be written on integralform as:

$$\oint_C \bar{E}(t) \cdot d\bar{l} = -\frac{d\Phi}{dt} \tag{3}$$

where c is the curve that is enclosed by the conducting loop and Φ is the flux through the open surface that the loop encloses. The use of vector notation is important to calculate the equations for the correct phase and amplitude.

2.3.2 Induced voltage

The induced voltage V_{ind} over loops of conducting wires and conductive material can be calculated from the law of induction:

$$V_{ind} = -\frac{d\Phi}{dt} = \oint_C \bar{E}(t) \cdot d\bar{l} = -\frac{d}{dt}\iint_S \bar{B}(t) \cdot d\bar{s} \quad (4)$$

For a voltage to be induced, the area S must be an open surface. The induced voltage is the greatest when the normal vector of S is parallel or anti-parallel to the direction of $\bar{B}$ and is zero when they're perpendicular to each other (K. Cheng, 1989).

2.3.3 Induced currents

The induced currents from time-varying electromagnetic fields are produced in conducting wires and also in conductive materials. For a circular loop with resistance R, the current I is calculated from the induced voltage V_{ind} by Ohm's law as:

$$I = \frac{V_{ind}}{R} \quad (5)$$

R can be calculated from the resistivity ρ of the conductive material, its length l and the cross-section area A by:

$$R = \rho\frac{l}{A} \quad (6)$$

It is important to notice that the induced voltage will vary in time and the loop can be reactive. These reactive dependence can come from the capacitors and inductors in the implant circuitry that is connected to the receiver induction coil. When the currents are induced in the material itself and not only in conductive loops, they're called eddy currents. The eddy current is produced, according to Lenz's law which says that changes in magnetic fields are counteracted by induced currents with an opposite directed magnetic field (K. Cheng, 1989). In MRI applications the eddy currents are critical because they can be induced in patients, coils and probes. The risk for induced eddy currents is minimized by the use of gradient shielded MRI scanners. The eddy currents are dependent on object shape and size, frequency, magnetic flux density, resistivity and permeability. For some pulse sequences the maximum gradients of 40mT/m can have switching time of 50µs corresponding to 20kHz (C. Bushong, 2003).

2.3.4 Demagnetization

Demagnetization happens when a strong external magnetic field is applied to a magnet in a direction different from its magnetization-direction, creating a torque that wants to turn the magnets' polarization. If the magnet is fixed and can't align with the magnetic field it will at some extent be demagnetized. Some magnets are more easily demagnetized than others and how easily a magnet is demagnetized is given by its so called coercive force. The coercive force is defined as the strength in an external magnetic field at room temperature that has to be applied anti-parallel to the magnets magnetization in order to demagnetize it totally. To magnetize a magnetic material, or in other words to create a magnet, an external strong magnetic field is applied to the magnetic material under very high temperature. This will give the magnet a certain magnetization that is remained when the temperature is decreased back to normal room temperature and the external magnetic field is removed. The magnetic flux density that the magnet has at this time is called the remanence flux density. In hearing implants, permanent magnets with a remanence flux density over 1 T are

used. In the MRI environment, the strong static magnetic field of the MRI scanner have the power to magnetize and demagnetize magnets at room temperature and even more easily if the implant gets heated. Magnetization is not a problem since they will only get stronger of that, but demagnetization is a problem because the magnets will lose their power and thereby their function. For magnets to avoid being demagnetized they have to be designed in a way that all the magnetization directions of the magnets has the possibility to move freely and align with the fields from the MRI scanner (K. Cheng, 1989).

2.3.5 Forces

In studies of movement, force and torque on cochlear implants, the internal magnet has shown to be the main cause to these effects (Teissl et al, 1998). When looking at forces of the internal magnet during MRI scanning, there are mainly three types of forces to consider:

- The pulling force F_{pull}
- The maximum rotational force F_{rot}
- The gradient field force F_{grad}

The pulling force wants to pull the magnet towards the area around the iscocenter of the scanner where the static magnetic field is homogenous. Once the magnet has reached this area, the pulling force will no longer be present. This is because the magnetic field strength is highest in this area and as long as the magnet is at a certain distance from it, where the magnetic field strength is lower, it will always be subject to this force according to:

$$F_{pull} = m\frac{\Delta B}{\Delta z} \tag{7}$$

where m is the magnetic moment of the magnet and ΔB is the difference in magnetic flux density for a distance Δz (Shellock et al, 2005). The contribution from forces in x- and y-direction has been neglected as the patient is assumed to enter the scanner in the z-direction.

The magnetic moment of an object of magnetic material in free space can be calculated as:

$$m = \frac{BV}{\mu_0} \tag{8}$$

where B is the magnetic flux density of the object, V the object volume, and μ_0 the permeability in free space.

The maximum rotational force is strongest force and will occur when the magnetization direction of the magnet is different from the direction of the static magnetic field direction. This will make the internal magnet rotate to align with the field direction of the scanner and can be painful to the patient or damage the implant (Teissl et al, 1998). The maximum rotational force comes from the maximum torque T_{max} which is achieved when the magnet's magnetization direction is perpendicular to the direction of the static magnetic field:

$$T_{max} = mB_0 \tag{9}$$

where m still is the magnetic moment of the magnet and B_0 is the flux density of the static magnetic field. In order to express this as a maximum force on the magnet, the maximum torque is divided by the diameter of the magnet. This force is further referred to as the maximum rotational force.

The gradient field force is the smallest of all the three forces for the internal magnet. Even though it can lead to vibrations and heating of other metallic and ferromagnetic materials of larger size than the magnet, in the case of cochlear implants this force is neglected compared to the pulling and maximum rotational force (Teissl et al, 1998). This force can be calculated similar to the pulling force. The only difference is that the magnetic field from the gradient switching varies with time and produces eddy currents, which has to be neglected. Sometimes the eddy currents in conductive materials are too big to neglect and need more complicated calculation. The time-varying fields will also create vibrations in the material.

2.3.6 Image Artifacts

Artifacts from magnets and objects will be presented in the image close to the magnet as darker area, but also as a misinterpretation of shapes and geometry. The reason for the artifacts is differences in magnetic permeability. If the permeability in the implant is greater than in tissue, the implant will interact with the gradient fields because it gets magnetized. The permanent magnets in the implant already have a magnetization and will therefore interfere with the gradient fields even if they have permeability close to tissue. If the magnet gets demagnetized in the MRI scanner before the scan begins, the artifacts from that magnet will decrease. The interference with the gradient fields occurs in such a way that the Larmor frequency will change in the area where the magnetization occur. For the imaging to work properly, the gradient fields have to be linear, but the magnetization makes the gradient fields non-linear. This will result in a misinterpretation of geometry such as anatomical position and shape (Carlsson, 2009).

2.3.7 Heating

Heating of medical implants in a MRI scanner is caused by induced currents from RF fields and pulsed gradient fields. The reason for the heating of these fields is that they induce eddy currents in electrically conductive materials. The eddy currents arise when a magnetic field varies with time, which characterizes these fields. For conductive and metallic implants with sharp edges, wires and closed loops the currents will occur more easily. These currents can also lead to vibrations and at some levels to nerve stimulation or interference with active implants (Shellock et al, 2005). For the RF fields, long wires will act like RF receiving antennas and the longer the wire is the greater will the change in magnetic field over the wire be, which will result in higher current density. How much the wire acts like an antenna will also depend on the Larmor frequency and the wave-length of that frequency. The Larmor frequency and wave-length will depend of the static magnetic field density, see Table 3-1.

Static field B_0 (T)	Larmor Frequency f (MHz)	Wavelength λ (m)
0.2	8.5	24.7
0.3	12.8	16.4
1.0	42.6	4.9
1.5	63.9	3.3
3.0	127.7	1.6
9.4	400.3	0.5

Table 2-1: Larmor frequency and wavelength in tissue for typical static magnetic fields. Heating of implants is dependent on the implant geometry and the wave-length of the transmitted RF pulse (Shellock, 2007).

The wavelength has been calculated according to:

$$\lambda = \frac{c}{f} = \frac{0.7c_0}{f} \quad (10)$$

where f is the Larmor frequency, c the speed of light in tissue and c_0 the speed of light in vacuum (Nordling and Österman, 2006). The stronger the static fields of today's MRI scanners, the smaller the metallic parts or wires need to be to act like antennas and heat the implant. The static magnetic field of 9.4T will have a wavelength of 0.5247 m and if the wire is of that length or longer, it will collect electrical charges at its edges that can lead to heating of the surrounding tissue. Today, the risk of induced temperature because of induced currents has shown to be insignificant compared to other implications on cochlear implants during MRI scanning (Todt et al, 2010).

2.4 Magnets and other magnetic materials

As mentioned earlier, the electromagnetic fields of the MRI scanner will interact with magnetic materials. The interaction will be different depending on the magnetic properties of these materials. Magnetic materials can be divided into three groups, diamagnetic, paramagnetic and ferromagnetic. What characterizes the groups is how they react in terms of relative permeability when they're exposed to external magnetic fields.

Diamagnetic $\mu_r \leq 1$

Paramagnetic $\mu_r \geq 1$

Ferromagnetic $\mu_r >> 1$

When a magnetic field is applied to a diamagnetic material it will create an opposite directed magnetic field in itself. This will create a repulsive force on the material. Paramagnetic and ferromagnetic materials are similar and create a magnetic field in the same direction as the applied field. The only difference is that the ferromagnetic material shows more of this property and creates a stronger magnetic field than a paramagnetic material.

Properties of magnetic materials are sometimes shown in so called magnetization curves (K. Cheng, 1989). Permanent magnets is said to be hard magnetic materials, because they have their own magnetic field when the external magnetization field is removed. Soft magnetic materials only have a magnetic field as long as it's exposed to an external field, these materials are ferromagnetic with very high permeability (Boll, 1979). The transducer of the BCI has both permanent magnets and soft magnetic material, while the holding housing only has permanent magnets.

3 Material and Method

3.1 Literature study

A literature study was made to get an understanding of what had been done earlier in this research area. Scientific reports and books about MRI and implants where found at the library of Chalmers Technical University. Participation at lectures in the basics of MRI was also done.

3.2 Experiment

3.2.1 Sahlgrenska experiments

The purpose of the experiment was to discover the behavior of the holder magnet in the internal part of the BCI system in terms of image artifact, movement and demagnetization. SmCo and NdFeB magnets where used. For the demagnetization measurements, the magnets' magnetizations were measured before and after they were scanned at Sahlgrenska University Hospital. The demagnetization was then given by a ratio in percent as the magnetization after the scanning divided by the magnetization before scanning. The demagnetization was believed to depend strongly on the angle of which the magnet is entered into the scanner. This was relative to its magnetization direction and the direction of the static magnetic field of the MRI scanner (Majdani et al, 2008). A pulling force when entering the scanner was also expected, as in (Teissl et al, 1998) where maximum torque was measured at 941 mm from the isocenter. Homogeneity is achieved only inside the scanner at a marginally distance from its isocenter where the scanned object is supposed to be positioned during a MRI scan. Once the magnets were inside the scanner the maximum rotational force was measured. The time-varying fields were expected to make the magnet vibrate, but it was also investigated if it was the static field or the time-varying field that contributed the most to the demagnetization.

Before the experiment, a safety control was needed to be 100% safe that no accidents could happen and that the MRI scanner did not get damaged. If the small magnets could get dropped they could easily stop the operation of the MRI scanner for days, which would be a problem since the scanner is frequently used for scanning of patients. Therefore when measuring the movement of the internal magnet it was positioned in a small plastic box from which the movements were studied. For the torque measurements the expansion of a silicon band connected to the plastic box was used to measure the maximum rotational force and pulling force of the magnets. It was also tested if a soft magnetic material could be used to minimize the movement and keep the magnet in position. The purpose was to investigate if that material could be used together with a compression band to keep the internal part of the BCI in place. Disadvantages may be increased image artifacts and more forces due to the magnetic properties of the high permeability material. After the experiment it was possible to tell what type of holder magnet that is most suitable to use as internal holder magnet in terms of MRI.

The experiments at Sahlgrenska was done at two different dates, 2011-04-28 and 2011-05-27 with two different scanners, but both with 1.5T. The scanner used for the first experiments were a Philips Achieva and the other was a Horizon K4. The Horizon K4 had shielded the area around the scanner so it dropped from 1.5T to 0 very rapidly. The Philips Achieva did not have this function, which means that the force measurements will be different when entering the scanner. For implants, this slow

change in magnetic field strength will mean a smoother pulling force and might not be so unpleasant for the patient.

3.2.2 Demagnetization

The magnets used in the experiments for holding magnets were permanent disc magnets. For the demagnetization measurements the magnets were exposed to both the static magnetic field and time-varying fields of the scanner. The dependence of different angles such as perpendicular, parallel and anti-parallel to the static magnetic field were tested. The SmCo magnets were expected to be demagnetized less than the NdFeB magnets because they have higher coercivity and are therefore more magnetically stable, see table 3-1.

Material	Remanence flux density B_r (T)	Coercive Force H_c (kA/m)
NdFeB	1.17-1.21	≥995
SmCo	1.00-1.08	≥1990

Table 3-1: Remanence flux density and coercive force of the SmCo and NdFeB magnets used in the experiment.

For the measurement on the internal holding magnet, there were totally three disc magnet types with different size and magnetization. They have been given the names magnet A, B and C as in table 3-2.

Magnet type	Material	Diameter X Thickness (mm)	Magnetization direction	Flux density (mT)
A	NdFeB	10 X 2	Axial	300
B	SmCo	8 X 3	Axial	290
C	NdFeB	14.5 X 4.5	Diametral	450

Table 3-2: The different properties of magnet types A, B and C.

3.2.3 Forces

The force measurements were done on the pulling and maximum rotational force. For the pulling force a NdFeB magnet with magnetization over its diameter (diametral) was used and for the maximum rotational force an SmCo magnet with axially magnetization were used. The reason for having an SmCo magnet when measuring the maximum rotational force was that it was expected to be more resistant against demagnetization than the NdFeB magnets. If demagnetization occurs during the measurement it will affect the results. The measurement setup for the maximum rotational force is shown in Figure 3-1 and the pulling force in Figure 3-2. The forces for both rotational and pulling were measured as a function of the expansion of a silicon band. The expansion length was translated into a force by the use of a Newton-meter. For the pulling force the expansion length of the silicon band was measured directly, but for the maximum rotational force the lifting height of the box was measured and then the expansion length was calculated according to:

$$\Delta L = \sqrt{h^2 + \left(R - \sqrt{R^2 - h^2}\right)^2} \quad (11)$$

$L = 6\ cm$ and is the start length of the silicon band when there is no pulling force in it. ΔL is its additional length due to the pulling force. h is the lifting height with which the box rises in the x-plane of the MR scanner. $R = 5.5\ cm$ is the length of the box. The angle θ between the static magnetic field direction and the magnet's magnetization direction was calculated as:

(12) $\theta = \cos^{-1}\left(\frac{h}{R}\right)$

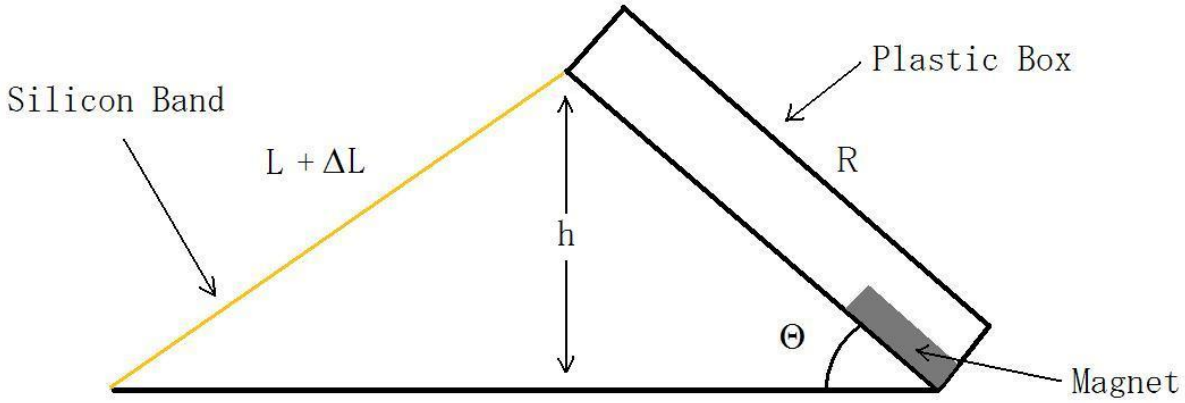

Figure 3-1: The maximum rotational force measurement setup. The magnet is put inside a plastic box that stretches a silicon band as the magnet wants to rotate.

Figure 3-2: The pulling force measurement setup. The silicon band gets stretched when the magnet is pulled towards the isocenter of the scanner.

3.2.4 Image Artifacts

To be able to locate the regions of image artifacts the magnets where placed on a phantom head filled with a saline solution and contrast agent gadolinium to give it the same relaxation time as for brain tissue. The phantom had a grid made up by small plastic cylinders to give more detailed information of the geometrical dispersion of the artifacts. The small dots in the resulting image will change their shape when they're close to the magnet and this type of phenomenon is not possible to detect without the grid. The phantom head is of cylindrical shape and is illustrated in Figure 3-3. It has a height and diameter of 95 mm and 380 mm respectively and the distance between the dots from their center is vertically and horizontally 50 mm. For the imaging, the magnets were positioned in the center of the phantom with their magnetization direction perpendicular to the direction of the static magnetic field of the scanner. The images were obtained for three different types of pulse sequences for both the SmCo type B magnet and the NdFeB type A magnet. The pulse sequences were Spin Echo (SE) with high bandwidth, Gradient Echo (GE) T1 weighted fast field echo (T1W.FFE) and an Echo Planar Imaging (EPI) SE sequence.

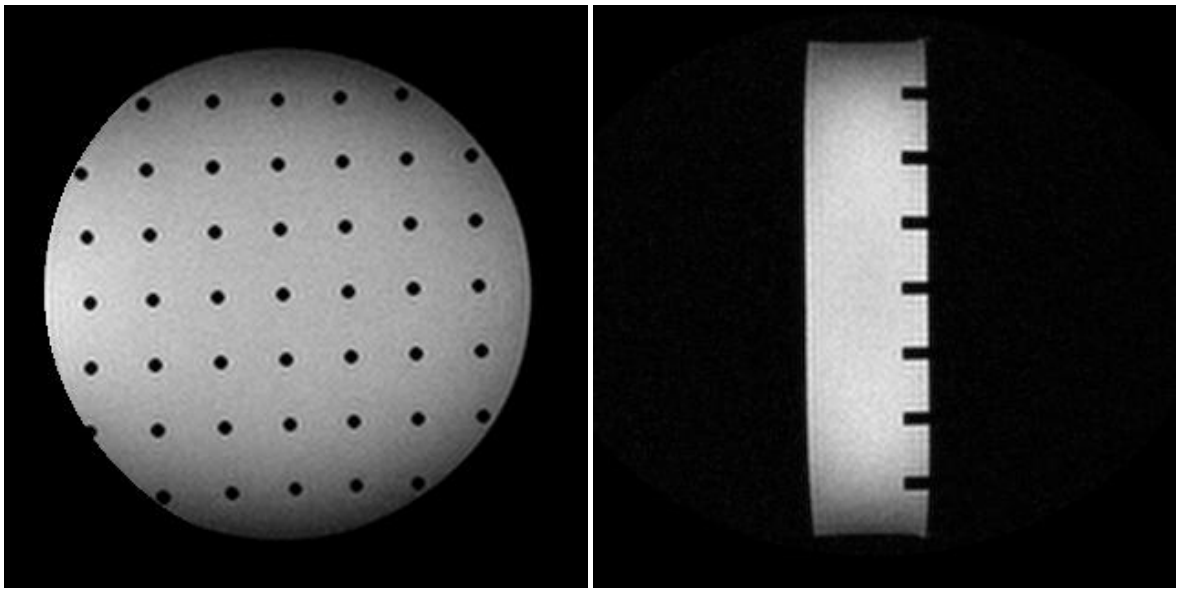

Figure 3-3. Images taken on the phantom without magnet. Sagittal view to the left and coronal view to the right.

3.2.5 Shielding

In order to see if it was possible to remove the maximum rotational force by the use of a soft magnetic material, a mu-metal plate was positioned under the magnet. The mu-metal had the purpose to shield the magnet by letting the flux density be higher in the plate than over the magnet. See figure 3-4 for the measurement setup. Two mu-metal plates of different sizes were tested, one smaller and one bigger, both of thickness 1.5mm. The small had an area of 15X15mm and the big plate 40X55mm. The idea was to use the mu-metal plate together with a compression band to remove forces on the implant during MRI.

Another shielding experiment was done on the transducer. It was evaluated if the soft magnetic material in the transducer could shield the transducer magnet from getting demagnetized. The transducer magnet's flux densities was measured before and after being exposed to the MRI scanner. The soft magnetic material in the transducer has a saturation flux density over 2.35T and a relative permeability over 12000. In this experiment the transducer was fixed inside a plastic box that in such a way that the magnetic fields of the scanner interacted with transducer as if it was positioned on a patient.

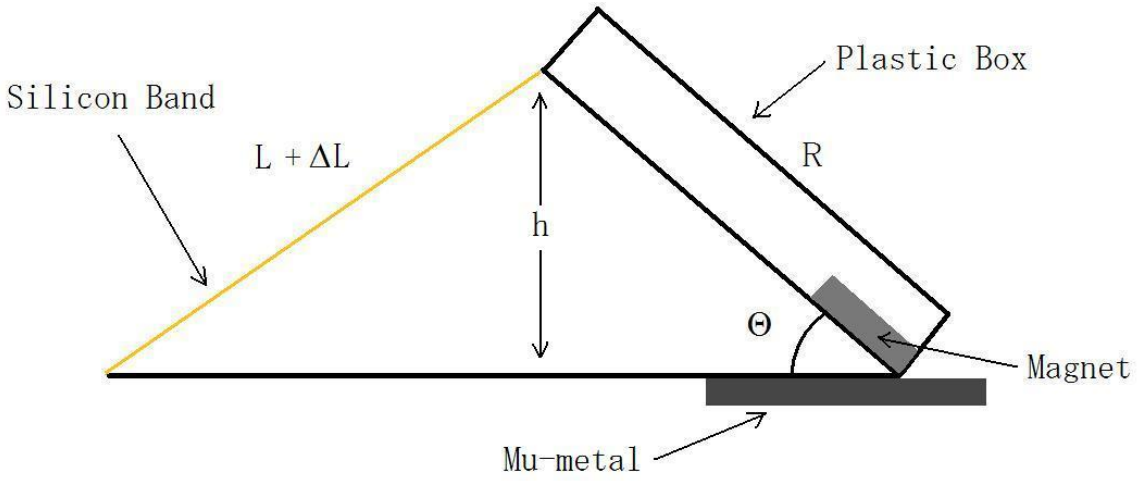

Figure 3-4: The measurement setup for rotational measurements with mu-metal. The mu metal was used in an attempt to prevent the magnet from rotating.

3.3 Simulation

COMSOL Mustiphysics has been used to simulate different parts of the implant with the purpose of explaining what happens in the reality when the implant is in the MRI environment in terms of demagnetization, mechanical force and other possible physical phenomenon that might occur. In the simulation it is possible to change physical parameters and see how it will affect the result. With this information it is easier to explain what happens in the real world and then being able to compare theory with experimental results. During the time since research begun in the field of MRI and medical implants, there has been significant experimental work done in the area leading to amazing breakthroughs and discoveries. By the use of today's advanced computer technology it is possible to simulate the same things and discover things that earlier wasn't possible.

All the simulations had the purpose to simulate the soft magnetic material around the transducer in terms of magnetic flux density. The principle is that the soft magnetic material has higher relative permeability than all the other components. This will make the flux density higher in that material and lower in the other materials with lower relative permeability. An example of what this would look like is shown in Figure 3-5 where a high permeability material is surrounded by air in a homogenous magnetic field. The "Surface" shows the absolute value of the magnetic flux density. The flux density is highest in the soft magnetic material, shown by red color and the blue color around it indicates that it's very low around it. The external applied field goes from left to right. The arrows show the way that the magnetic flux density will take through the soft magnetic material. The axis shows the width and height of the object.

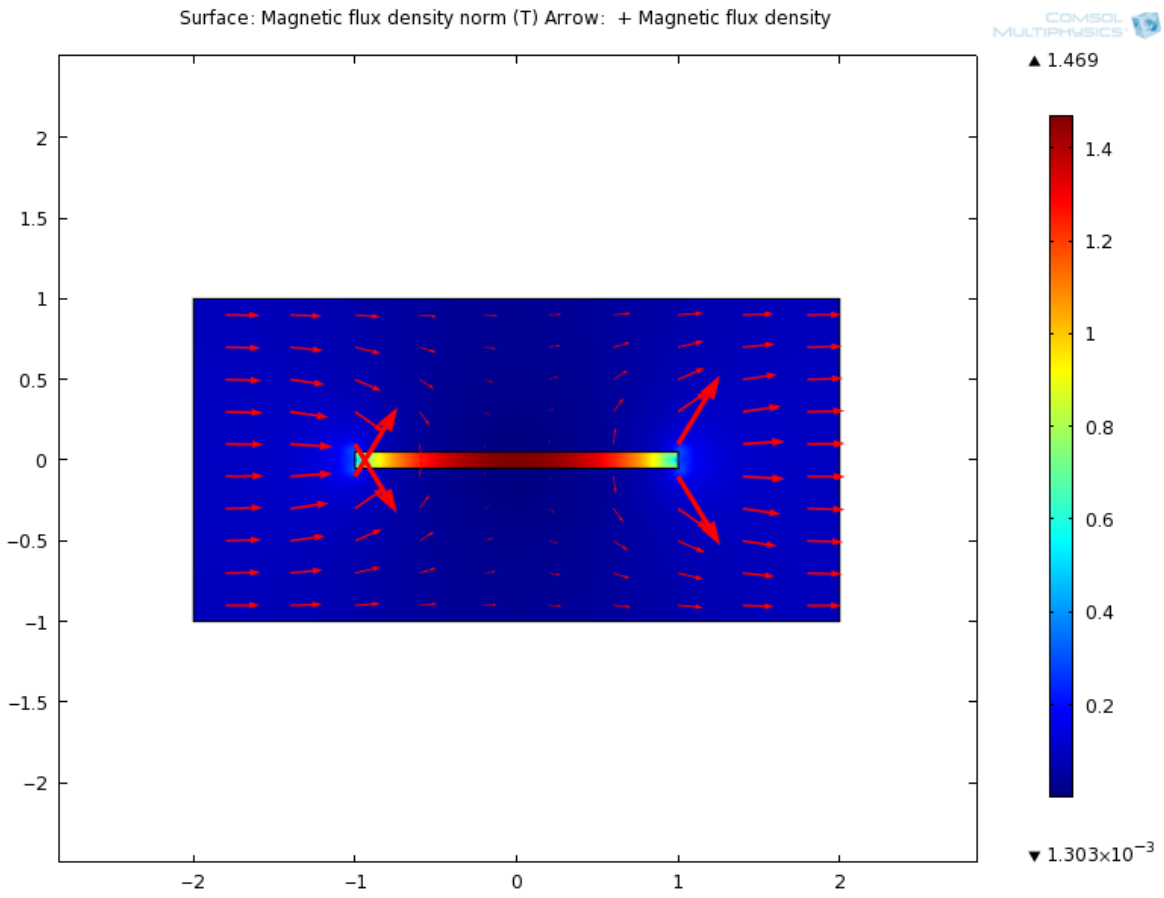

Figure 3-5: A high permeability material surrounded by air in a homogenous magnetic field, simulated in COMSOL Multiphysics. The flux density is higher in the soft magnetic material, because it has a higher permeability.

4 Results

4.1 Experiment

4.1.1 Demagnetization

The magnetization of some magnets was measured before and after they were exposed to the fields of the scanner. The magnets were measured at Sura Magnets and Imego, see table 4-1 and 4-2 respectively for these results. Totally 8 magnets were exposed to the scanner at different angles and for different time. At Imego the magnets' magnetic flux density was measured with a Gaussmeter Lakeshore 421. At SuraMagnets another measurement method was used that measured the magnetic flux of the magnets. The magnetic flux measurement is an accurate method, because it gives information of the whole magnet's magnetization. The magnetic flux density measurements with the Gaussmeter only gives the magnetic flux density at one point of the surface of the magnet.

Magnetic flux before MRI (10^{-5} Vs)	Magnetic flux after MRI (10^{-5} Vs)	Demagnetization (%)	Exposed to pulse sequence	Magnetization direction relative to the static magnetic field	Material
111	10	91	Yes	Perpendicular	NdFeB (Type A)
102	100	2	No	Perpendicular	SmCo (Type B)
104	58	44.2	Yes	Perpendicular	SmCo (Type B)
102	102	0	Yes	Parallel	SmCo (Type B)
101	100	1	No	Parallel and Perpendicular (randomly)	SmCo (Type B)

Table 4-1: Demagnetization measurements of internal holding magnets. Measurements were done at SuraMagnets where the magnetic flux of the magnets were measured.

Magnetic flux density before MRI (mT)	Magnetic flux density after MRI (mT)	Demagnetization (%)	Exposed to pulse sequence	Magnetization direction relative to the static magnetic field	Material
450	460	-2.2 (increase)	Yes	Parallel	NdFeB (Type C)
272	4	98.5	No	Anti-parallel	NdFeB (Type A)
290	290	0	No	Anti-parallel	SmCo (Type B)

Table 4-2: Demagnetization measurements of internal holding magnets. Measurements were done at Imego where the magnetic flux density was measured.

4.1.2 Forces

The results from the maximum rotational force and pulling force measurements are shown in table 4-3 and table 4-4 respectively. The maximum rotational force for the SmCo magnet of diameter 8mm and thickness 3mm was measured to be 7.1N close to the isocenter of the scanner in the area where the static magnetic field strength is homogenous.

Distance from opening (cm)	**Height h (cm)**	**Additional length ΔL (cm)**	**Angle θ (Degrees)**	**Maximum rotational force (N)**
90	0	0	0	0
80	0.07	0.07	0.7	0.3
70	0.15	0.15	1.6	0.5
60	0.3	0.3	3.1	0.7
50	0.35	0.35	3.7	0.8
40	0.9	0.9	9.4	1.7
20	1.5	1.5	15.8	3.0
10	2.5	2.5	25.9	4.4
0	3.7	4.0	42.3	5.1
-10	4.3	4.8	51.4	5.7
-20	4.7	5.4	58.7	6.4
-30	4.9	5.8	63.0	6.7
-40	5.0	5.9	63.4	7.1
-50	5.0	5.9	63.4	7.1
-88 (isocenter)	5.0	5.9	63.4	7.1

Table 4-3: The results from the maximum rotational force measurements. The maximum measured maximum rotational force was 7.1N.

For the pulling force measurement the maximum measured force was 3.28N with a NdFeB (Type C) magnet of diameter 14.5mm and thickness 4.5mm at a distance 10 cm inside the scanner.

Distance from opening (cm)	**Additional length ΔL (cm)**	**Force (N)**
80	10.0	0.6
75	10.5	0.7
70	10.5	0.7
65	10.6	0.7
60	10.7	0.7
55	10.8	0.7
50	10.8	0.7
45	11.0	0.7
40	11.1	0.7
35	12.0	0.8
30	12.9	0.9
25	16.5	1.5
20	16.9	1.6
15	17.3	1.6
10	18.5	2.1
5	21.0	2.7
0	21.0	2.7
-5	22.0	3.1
-10	22.2	3.3
-15	22.0	3.1
-20	21.5	2.8
-25	20.0	2.7
-30	19.5	2.3
-35	17.5	1.6
-40	14.0	1.0
-45	12.0	0.8
-50	11.0	0.7

Table 4-4: Shows the measurement results on the pulling force. The maximum force was 3.28N

4.1.3 Image Artifacts

4.1.3.1 Spin-echo sequence with high bandwidth

The first images were taken with a SE sequence with a pixel bandwidth of 2990 Hz/pixel for sagittal and coronal views. See Figure 4-1 and 4-2. This sequence gives the smallest artifacts of the image and the sizes of the artifacts are concluded in table 4-5.

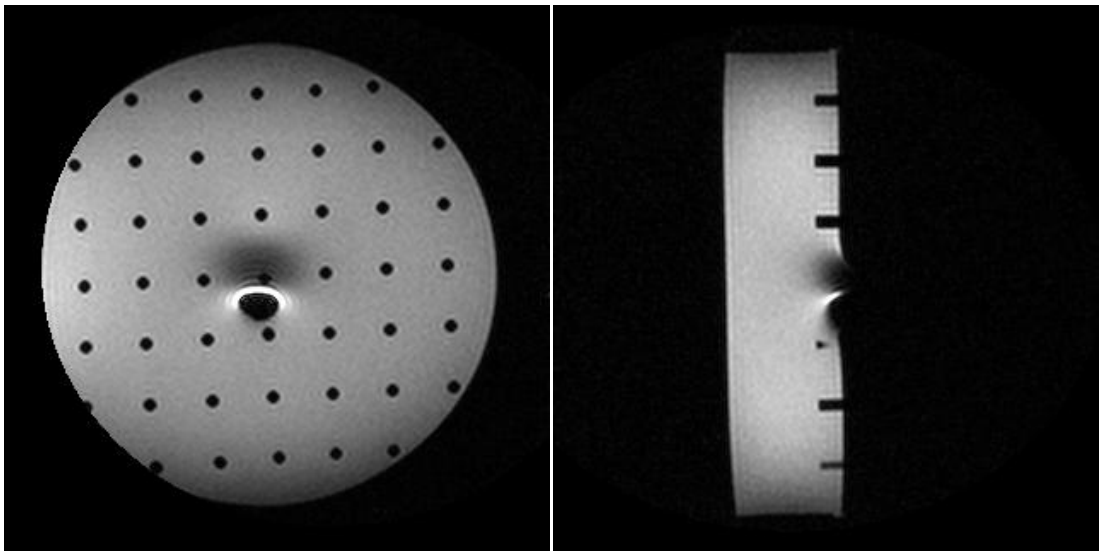

Figure 4-1: Image on the NdFeB magnet type A for a SE sequence with high pixel bandwidth. Sagittal view to the left and coronal view to the right.

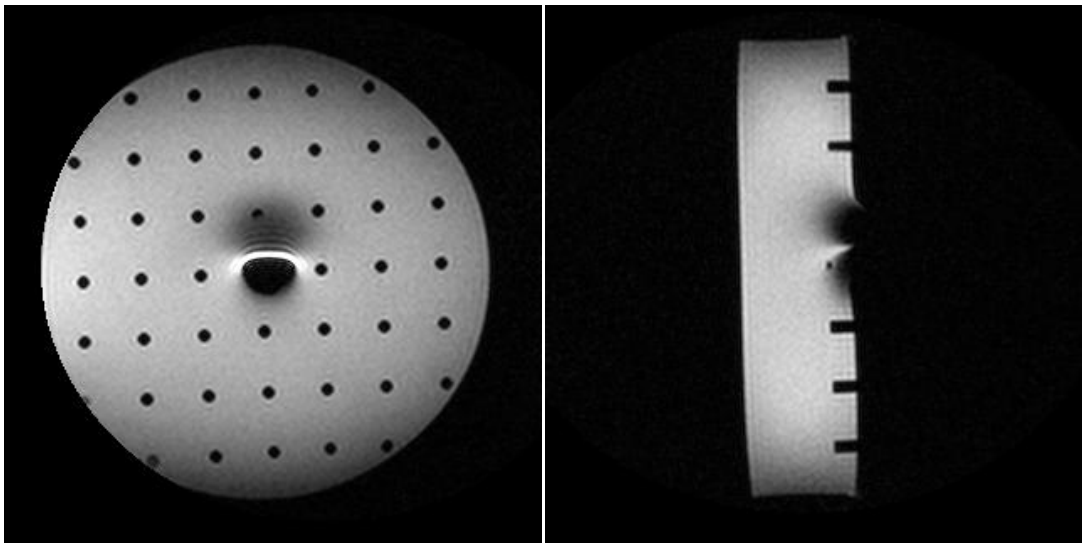

Figure 4-2: Image on the SmCo magnet type B for a SE sequence with high pixel bandwidth. Sagittal view to the left and coronal view to the right.

Magnet	Sagittal view (Circle diameter)	Coronal view (Rectangle width and height)
NdFeB (Type A)	70 mm	26 mm X 90 mm
SmCo (Type B)	90 mm	50 mm X 110 mm

Table 4-5: The image artifacts from NdFeB (Type A) and SmCo (Type B) magnets, scanned with a SE Sequence with high pixel bandwidth.

4.1.3.2 Spin-Echo EPI

In Figure 4-3 and 4-4 the same images are taken as in Figure 4-1 and 4-2, but with an EPI SE sequence with a bandwidth of 1250Hz/pixel resulting in a more distorted image. This sequence is a SE sequence called Echo Planar Imaging (EPI) and is a typical pulse sequence for imaging patients in applications that requires fast imaging times such as functional MRI. It can produce a complete image in 50ms (C. Bushong, 2003). This imaging sequence was the one in the experiment that distorted the image worst.

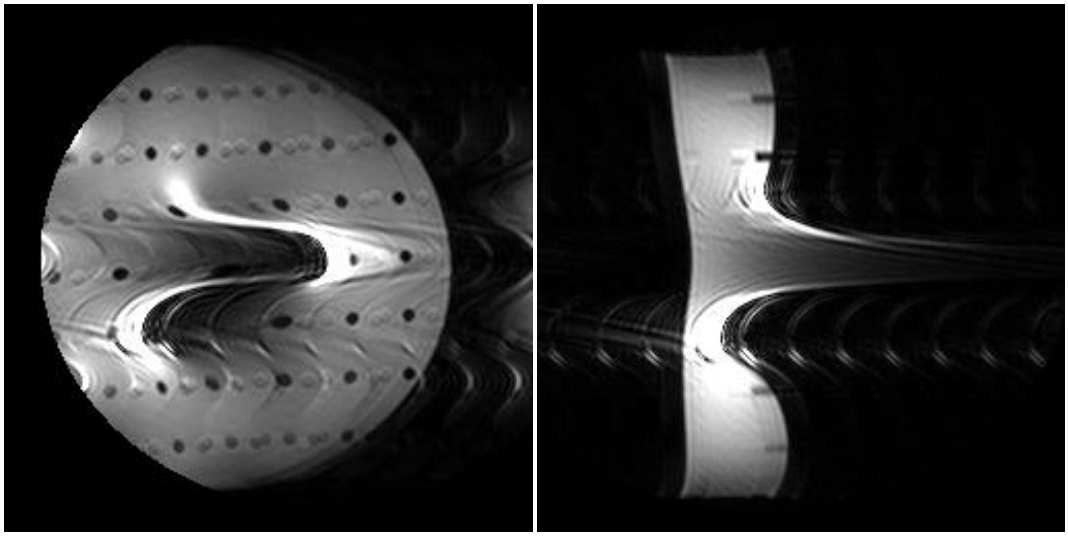

Figure 4-3: Image on the NdFeB magnet type A for a SE EPI sequence with low pixel bandwidth. Sagittal view to the left and coronal view to the right.

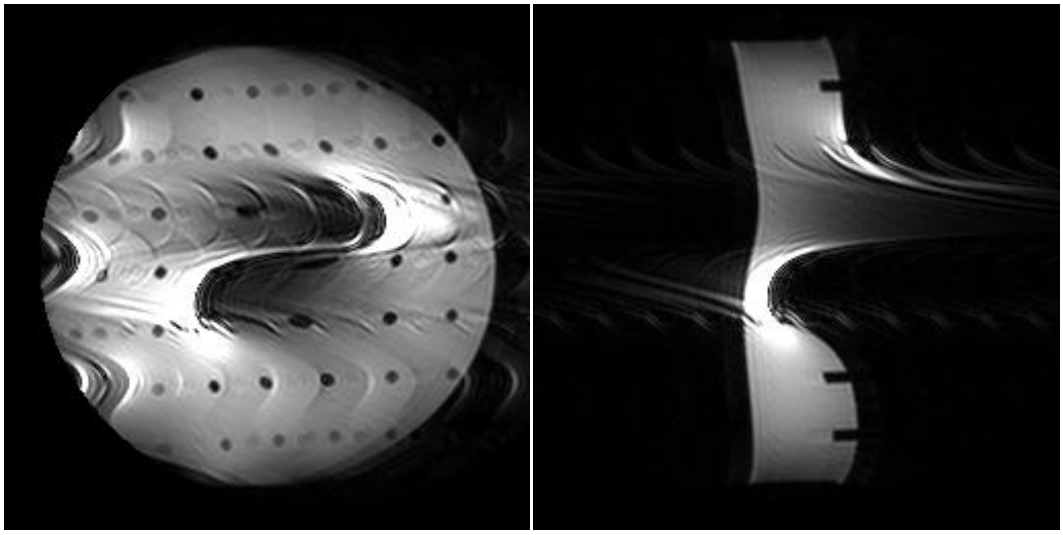

Figure4-4: Image on the SmCo magnet type A for a SE EPI sequence with low pixel bandwidth. Sagittal view to the left and coronal view to the right.

4.1.3.3 Gradient-Echo T1 weighted FFE

The sequence used in figures 4-5 and 4-6 is a GE T1 weighted pulse sequence called Fast Field Echo (FFE) and this is a typical pulse sequence used when imaging the heart (C. Bushong, 2003). The sizes of the artifacts are concluded in table 4-5. They're greater than the artifacts from the SE sequence with high pixel bandwidth, but lower than in the SE EPI sequence.

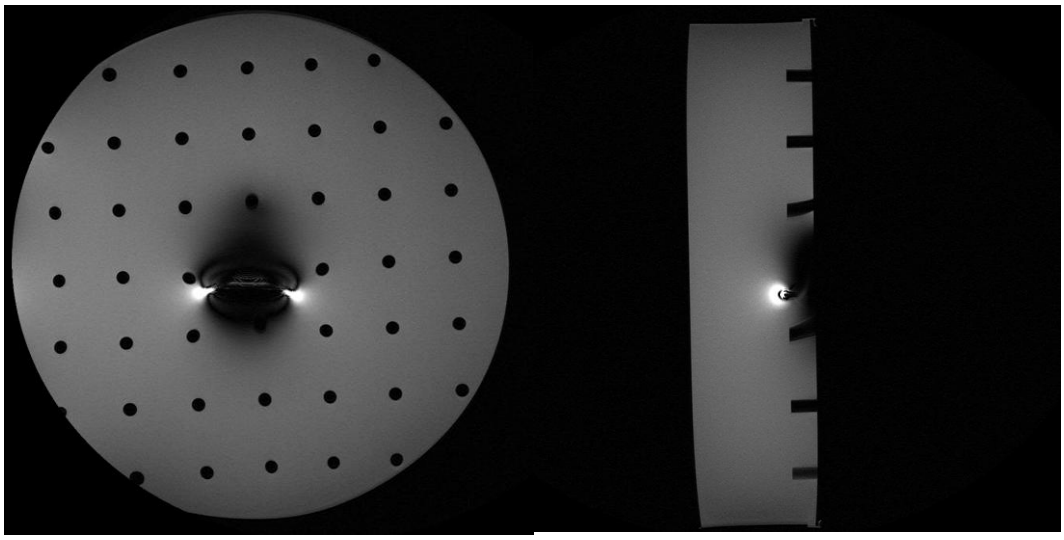

Figure 4-5: Image on the NdFeB magnet type A for a T1W.FFE sequence. Sagittal view to the left and coronal view to the right.

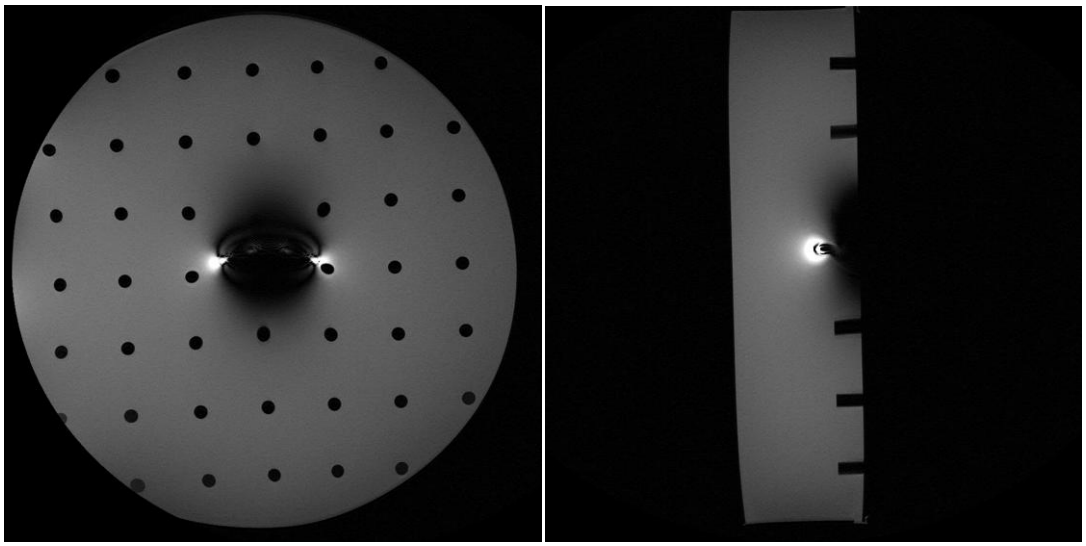

Figure 4-6: Image on the SmCo magnet type B for a T1W.FFE sequence. Sagittal view to the left and coronal view to the right.

Magnet	Sagittal view (Circle diameter)	Coronal view (Rectangle width and height)
NdFeB (Type A)	150 mm	45 mm X 140 mm
SmCo (Type B)	175 mm	75 mm X 165 mm

Table 4-6: Image artifact for the T1W.FFE image sequence.

4.1.4 Shielding

The magnet together with the mu-metal plate did not manage to keep the magnet in position. Movements were observed and the maximum rotational force was still the same with as without a

mu-metal plate. Additional forces were observed on the mu-metal plates since they are ferromagnetic.

For measurements on shielding of the transducer magnet another soft magnetic material was used instead of the mu-metal. This material had higher saturation flux density and relative permeability. The magnets demagnetization was measured and the results are concluded in the table 4-7. Two transducers were tested. During the experiment, one of transducers (Transducer 1) got destroyed because it wasn't fixed good enough inside the box and the static magnetic field of the scanner ripped it apart with so much power that one of the transducer magnet got broken into two parts and is therefore not shown in table 4-7 with the other magnets. Transducer 2 was better fixed and the experiment on it went well. There are totally four magnets in each transducer and they are surrounded by the soft magnetic material. The magnetic flux density was measured on the south-pole of the magnets and with the measuring probe at a distance of approximately 0.5 mm. Before the magnets were exposed to scanner their magnetic flux densities were measured at Imego with a Gaussmeter Lakeshore 421. The magnetic flux density is very sensitive to the distance between the measuring probe and the magnet and it was difficult to get exactly the same distance of 0.5 mm for both measurements. The results then measured to vary between 40-42 mT for a distance of 0.5 mm, which is smaller than after MRI exposure.

Transducer	**Magnet 1 Flux density (mT)**	**Magnet 2 Flux density (mT)**	**Magnet 3 Flux density (mT)**	**Magnet 4 Flux density (mT)**
1	92	97	83	-
2	73	82	74	90

Table 4-7: The flux densities of the transducer magnets after being exposed to the MRI fields.

4.1.5 Vibrations

The vibrations were only observed and not measured. When the holding magnet was fixed inside the plastic box, no vibrations were observed. When it was not fixed, it was allowed to move freely inside the box and when the time-varying fields were applied vibrations were observed. For the soft magnetic material in the transducer, vibrations were observed in both cases when it was fixed and not fixed. It reacted more to the time-varying fields than the holding magnet did. What should shield the magnets from demagnetization was now creating vibrations.

4.2 Simulation

The parts of the implant that has been simulated here are the internally implanted holding magnet and the transducer of the BCI in the MRI environment. It is possible to see how the MRI scanner and the BCI interact with each other by studying the electromagnetic properties for the choice of parameters for all different geometrical shapes and material properties.

4.2.1 Shielding and Demagnetization

By the use of a soft magnetic material with high permeability in the transducer it is possible to let the flux density be high in that material and low over the magnets. This will shield the magnets from the magnetic fields of the scanner and thereby avoid demagnetization.

4.2.1.1 The holding magnet

The holding magnet were simulated for different angles in the MRI scanner and its magnetic flux density is shown in Figure 4-7. The top magnet has its magnetization direction from left to right, the

middle image has it from right to left and the bottom image has it from top to bottom. The coloring shows the absolute value of the magnetic flux density and the arrows the direction of it. The reason for this simulation is to later see what happens with the magnetic flux density of the magnets when they are exposed to a homogenous external magnetic field with magnetic flux density of 1.5 T. This magnetic field simulates the static magnetic field of a MRI scanner and the result is shown in Figure 4-8. The magnets have a remanence flux density of 1 T. The direction of the external magnetic flux density, going from left to right, is here anti-parallel to the top magnet, parallel to the middle magnet and perpendicular to the bottom magnet.

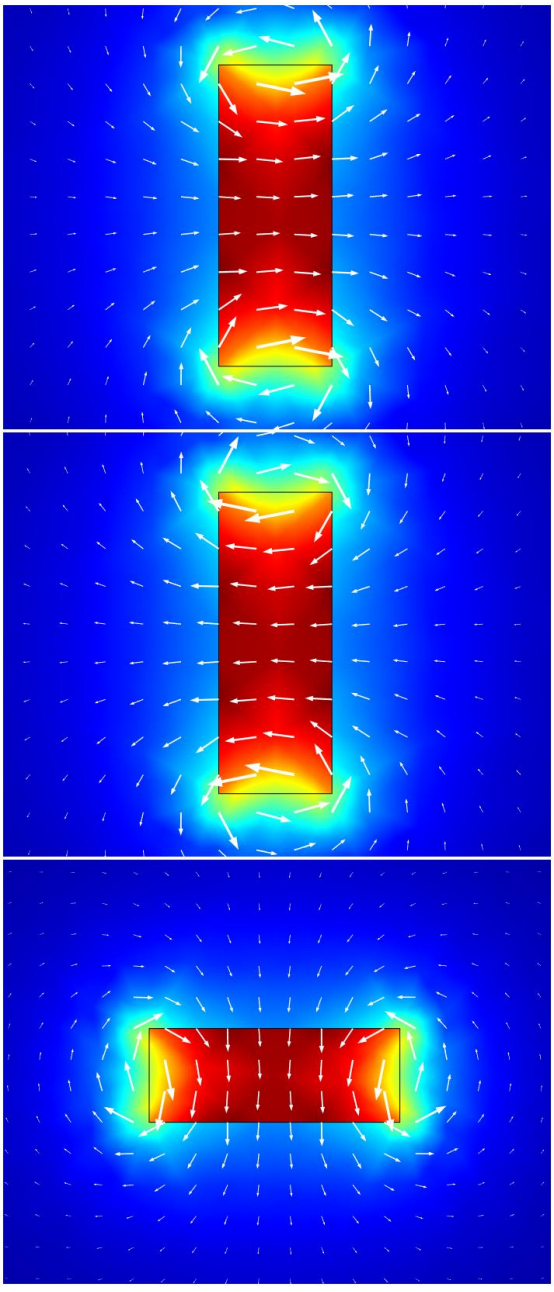

Figure 4-7: The magnetic flux density of the holding magnets at three different angles in relation to their magnetization direction.

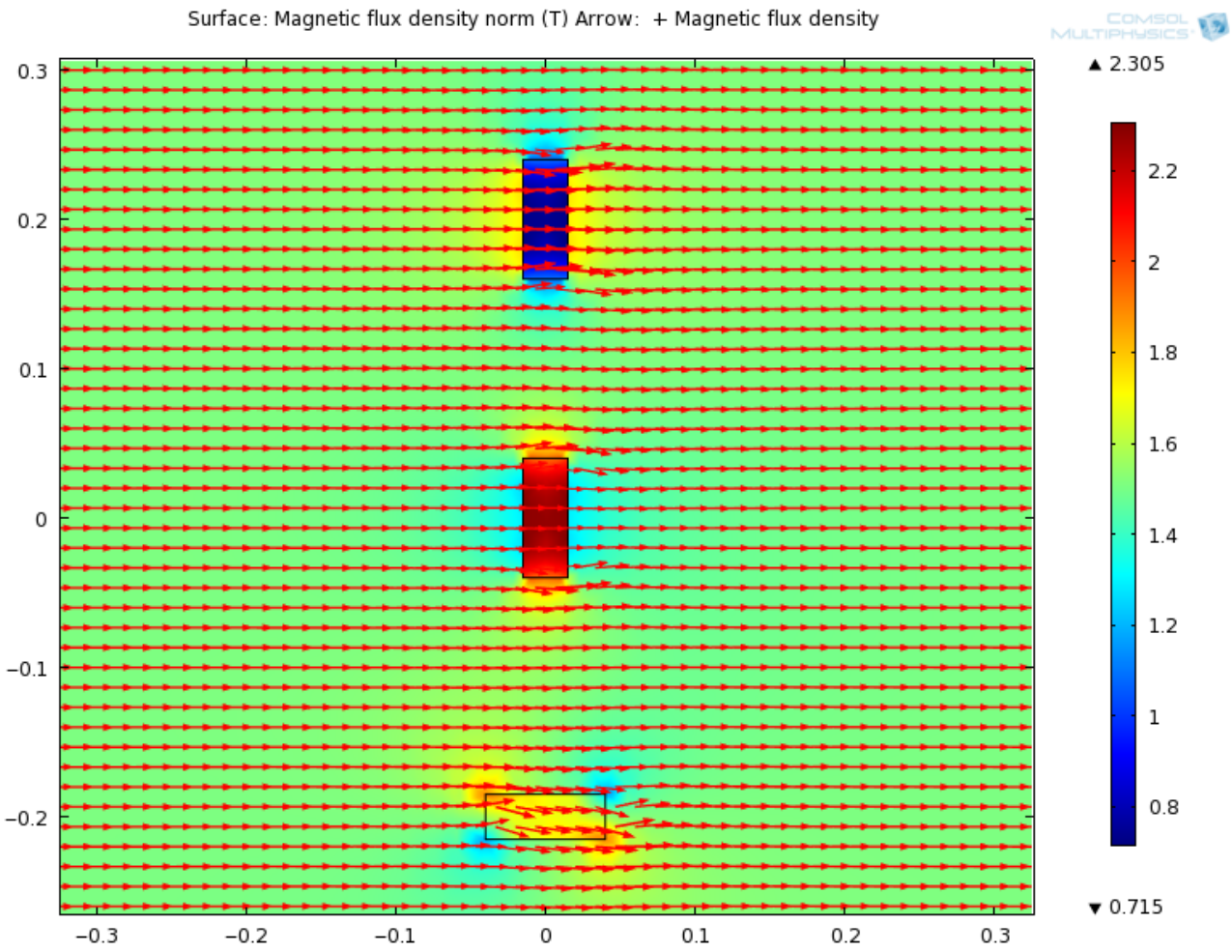

Figure 4-8: An illustration of the holding magnets when exposed to an external magnetic field for three different angles.

4.2.1.2 The transducer

The simulation of the magnetic flux density of the transducer, when exposed to the static magnetic field of the MRI scanner is shown in Figure 4-9 and 4-10. The transducer in these simulations is the transducer that was used in the experiments at Sahlgrenska University Hospital. All parts of the transducer are therefore not included in the simulations. In Figure 4-9 the angle between the transducer and the external field is the same as if it was positioned on a patient. This will shield the transducer's magnet from getting demagnetized since the flux density will flow in the soft magnetic material. To easier get an understanding of what has been simulated see Figure 4-11 and 4-12 where the magnetic flux density of the transducer have been simulated when no external magnetic field is applied. In Figure 4-12 the soft magnetic material of the transducer has been removed and the material surrounding the magnets has the same relative permeability as air.

The relative permeability of the soft magnetic material is around 12000, but when the flux density of the scanner is 1.5 T the material will be saturated. This means that the maximum flux density in the material will be saturated between 2-3T and the relative permeability is only 2.This is the case in figure 4-9 and 4-10. The remanence flux density of the magnets is 1 T and the external homogenous magnetic field has a magnetic flux density of 1.5 T.

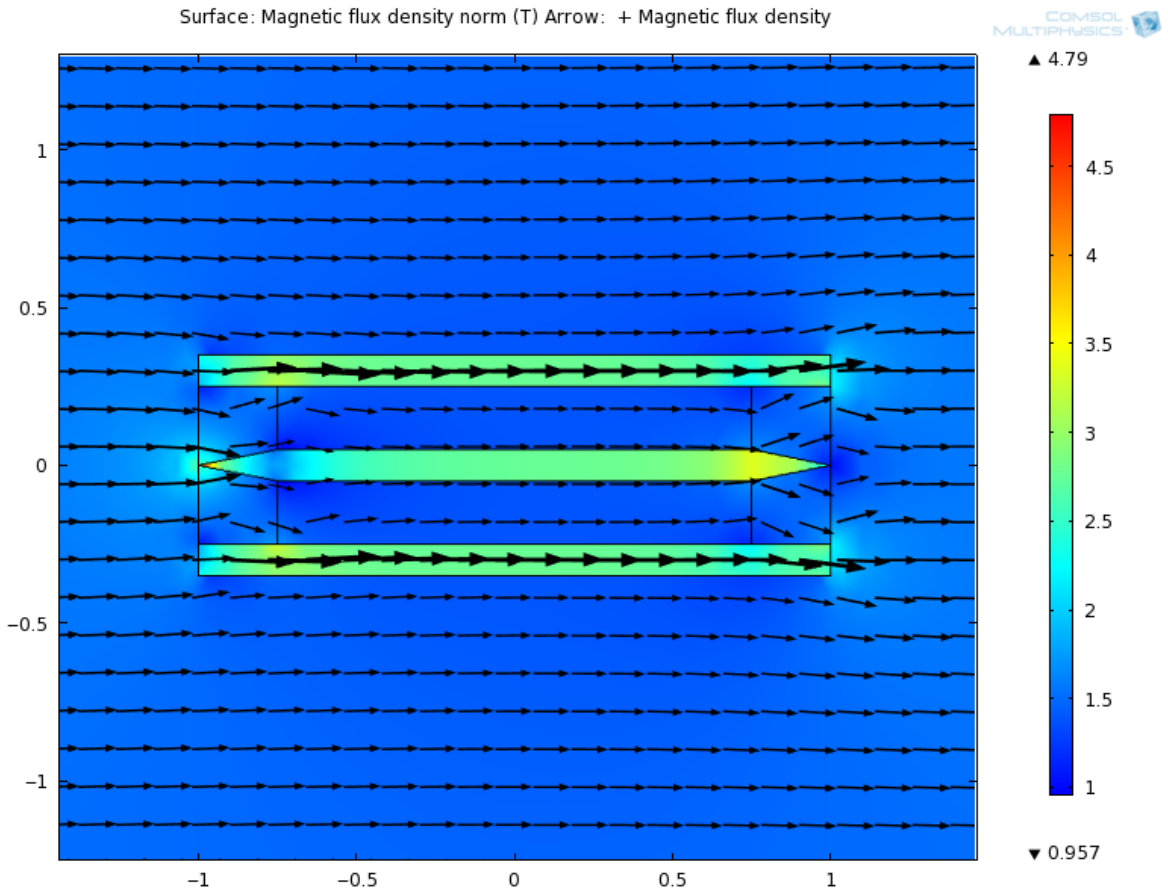

Figure 4-9: An illustration of the transducer exposed to the static magnetic field of the MRI scanner. The flux density from the scanner flows from left to right.

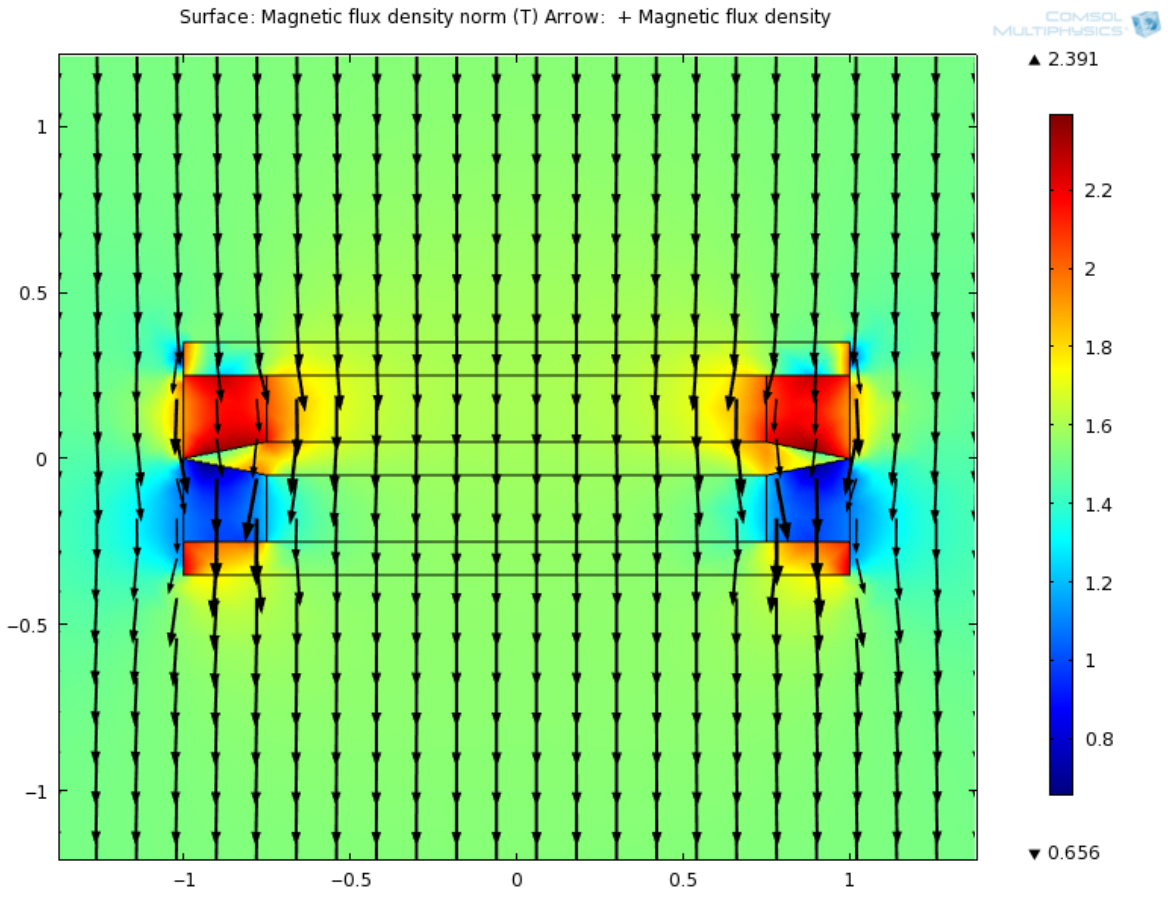

Figure 4-10: An illustration of the transducer exposed to the static magnetic field of the MRI scanner. The magnetic flux density of the scanner flows from top to bottom.

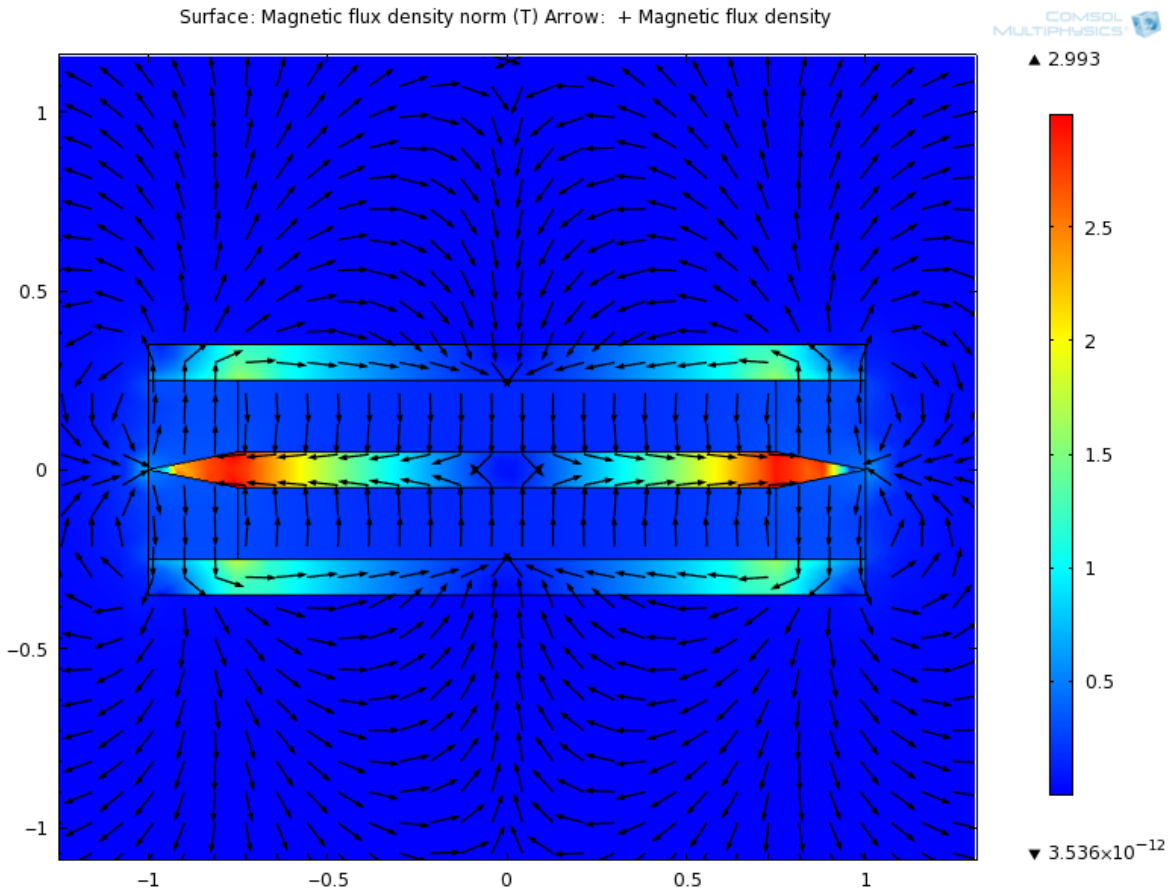

Figure 4-11. The magnetic flux density of the transducer, when no external magnetic field is applied. The length of the arrows are normalized to have the same length and therefore only shows the direction of the magnetic field.

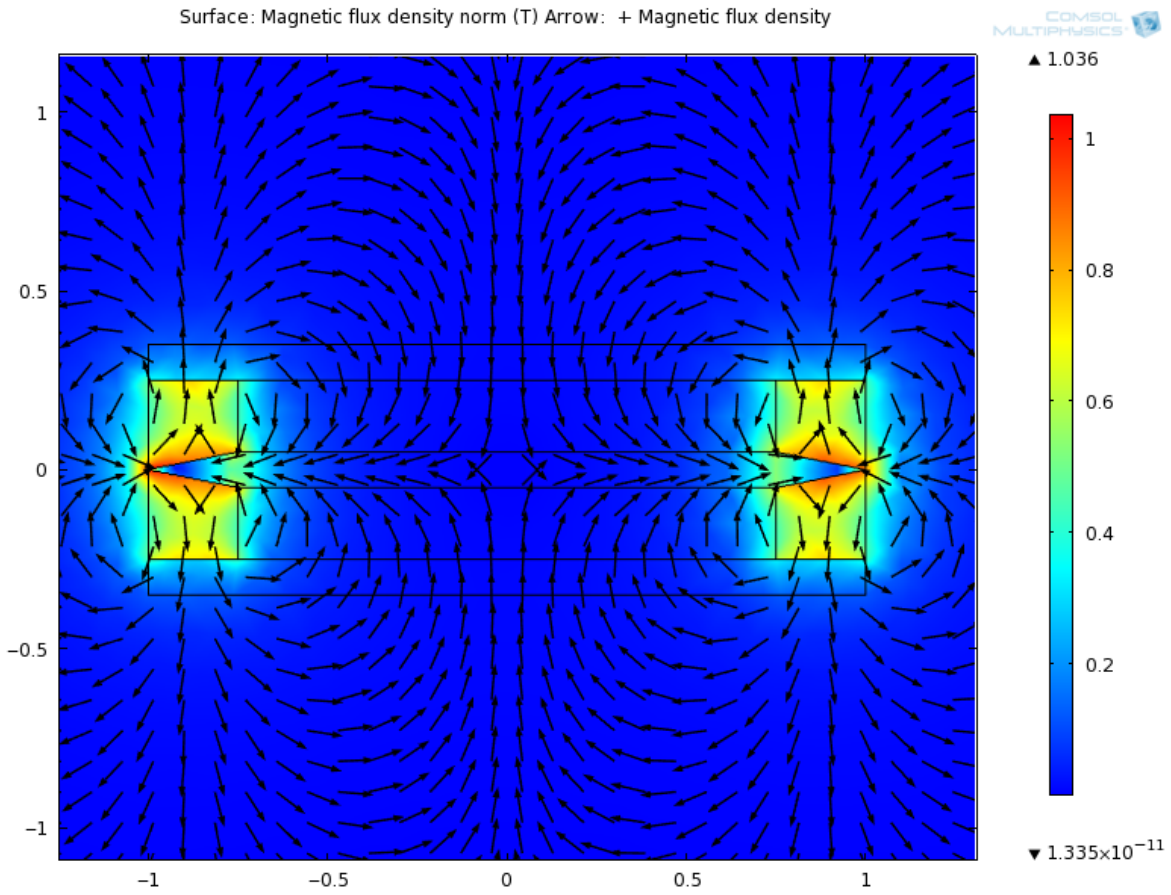

Figure 4-12. The magnetic flux density of the transducer when no external magnetic field is applied and the material surrounding the transducer magnets have the same relative permeability as air. The arrows lengths in the figure are normalized.

4.2.2 Heat generation

Objects with sharp edges tend to increase more in temperature, because it collects electrical charges at the edges where the electrical field has its highest intensity. By smoothening of the edges of the metallic and conductive objects the induced temperature will decrease significantly (Shellock, 2007). Figure 4-13 is a simulation of this phenomenon.

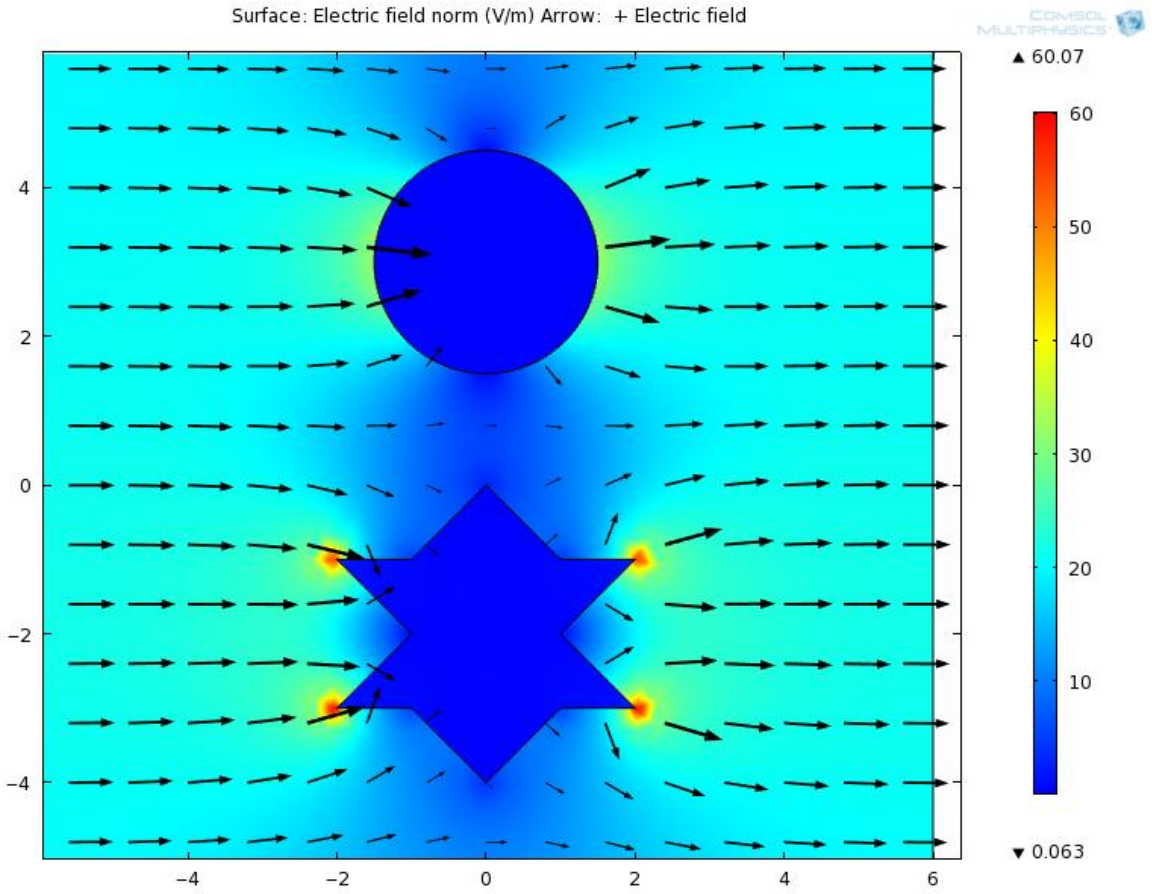

Figure 4-13. Simulation of an electric field interaction with an electrically conductive object. The intensity of the electric field will be higher at sharp edges (star) than at smooth edges (circle).

5 Discussion

5.1 Experiment

5.1.1 Demagnetization

The force between the holding magnets depends on the distance between the magnets and needs to be at least 0.3 N for 8mm thick skin and then the force for the same magnets will be 1 N for 4 mm thick skin(Teissl et al, 1998). If the magnets get demagnetized and lose some of its strength, then this force will decrease and the magnet might not manage to hold the parts together. The results obtained in table 4-1 and 4-2 shows that the demagnetization depends on the angle between the magnet's magnetization direction and the direction of the static magnetic field of the scanner. What's not clear from the experiment is if magnets that have been inside the scanner for a longer time will get more demagnetized. The problem is that the longest time that they've been inside the scanner is during the scanner time of about 3 minutes and then they've been exposed to time-varying fields for all tests. For some cases the magnets were inside the scanner even longer when imaging was done with more than one imaging sequence. No time tests were done on only the static field of the scanner.

The coercive force of the magnets is important to consider. It depends on the frequency of the time-varying field and temperature in terms of eddy currents. The higher the frequency, the higher the coercive force will be, which means that it will be more difficult to demagnetize the magnet. On the other hand, the reason for that is that induced eddy currents want to counteract the time-varying field by creating their own magnetic field in the opposite direction, according to Lenz's law. These eddy currents might heat the magnet and the higher the temperature is, the lower the coercive force will be (Boll, 1979). In order to tell something about the heating it has to be measured, which has not been done in this study since earlier research has shown that heating of the internal magnets has a significantly low effect (Shellock et al, 2005). Then the demagnetization only will depend on the angle and the time inside the scanner.

The functionality of the BCI transducer depends strongly on its magnets' stability and a demagnetization of these magnets will affect its performance significantly. The magnets in the transducer were almost fully shielded by the soft magnetic material around them. The holding magnets and the transducer magnets are both NdFeB magnets and since the holding magnets lost almost all of its strength without shielding, then the soft magnetic material must have shielded the magnets.

5.1.2 Forces

Earlier force measurements have been done on the holding internal magnet showing a maximum rotational force of 7.8 N and a pulling force of 0.29N (Teissl et al, 1998). When looking at force magnitudes on the internal magnet, it will depend on the volume of the magnet, see equation (8).

For the pulling and maximum rotational force measurements, magnets with different volume and material where used. This was not intentionally done and serves no purpose, but had to be so because of limited experimental time. However, that is not a problem since the force is proportional to the magnetic moment of the magnet so the force from one magnet can be used to calculate the force of another, this is yields both for pulling and maximum rotational force (Jesacher et al, 2010).

For example the force magnitude $\left|\vec{F}_{NdFeB}\right|$ on a NdFeB magnet with magnetic moment $\vec{m}_{NdFeB}$ can be calculated from the force $\vec{F}_{SmCo}$ measured on a SmCo magnet with magnetic moment $\vec{m}_{SmCo}$ as:

$$\left|\vec{F}_{NdFeB}\right| = \frac{|\vec{F}_{SmCo}|}{|\vec{m}_{SmCo}|}|\vec{m}_{NdFeB}| \quad (13)$$

The relation between the rotational and pulling force can be given by a ratio. It's important to notice that this ratio will be different for each type of scanner, depending on how fast the static field of the scanner goes from 0 outside the opening to 1.5T inside. This ratio can therefore only be used for calculation when the same scanner is used, which was not the case in the experiments at Sahlgrenska. However, the maximum rotational force will be the same for all scanners with the same static magnetic field. By using the data, obtained by Teissl 1998, the ratio r between the rotational F_{rot} and pulling F_{pull} force is:

$$r = \frac{|\vec{F}_{rot}|}{|\vec{F}_{pull}|} = \frac{7.8}{0.29} = 26.9 \quad (14)$$

This means that the maximum rotational force should be almost 27 times greater than the maximum pulling force for the type of scanner used in that experiment, which was a Magnetom Vision from Siemens Medical Systems. This scanner had an active shielded magnet, as the Horizon K4 in at Sahlgrenska, which means that the static field drops very rapidly outside the opening of the scanner (C. Bushong, 2003), thereby resulting in a higher pulling force.

The results of measurements of maximum forces are collected in table 5-1. By using these results together with equation (13) the pulling force and maximum rotational force could be calculated for any desired magnet. For a SmCo holding magnet of diameter 12.5 mm and thickness 2.25 mm the rotational and pulling force in the Horizon K4 will be 12.96 N and 0.78 N respectively. This gives the ratio $r = 16.51$ for the Horizon K4 scanner. For the Philips Achieva, the maximum rotational force would be the same, but the pulling force would be lower, since it has no active shielding. The pulling force will actually in reality be a little bit larger than calculated, since the magnet has a saturation magnetization value that is reached due to the applied field from the scanner. This will increase the magnetic moment of the magnet.

Force	Maxmum force (N)	Size Diameter X Thickness (mm)	Flux density (mT)	Material
Rotational	7.08	8 X 3	290	SmCo (Type B)
Pulling	3.28	14.5 X 4.5	450	NdFeB (Type C)

Table 5-1: Important values for calculating relations between the rotational and pulling force for different magnets and scanners.

5.1.3 Image Artifacts

If a soft magnetic material is used in the implant then the magnetization of that material will interfere with the gradients and the artifacts are expected to cover a big area of the image. If the artifacts cover a big area, then it might also be a problem to scan other parts of the body than the head.

The choice of image sequence will affect image artifacts a lot and a SE sequence with high pixel bandwidth gave the best results. The pixel bandwidth is the frequency that the received RF signal is sampled with. However, this image sequence is not used in clinical applications and is only used to

minimize the image distortions. The size of image artifacts for an image sequence that is used in clinical applications at Sahlgrenska University Hospital is concluded in table 4-6. These artifacts are not as small as for the high bandwidth image sequence, see table 4-5, but it is a sequence used in clinical applications. It also gives a better image than the SE EPI sequence where the artifacts cover the whole image.

5.1.4 Shielding

The shielding effect of the transducer magnets was measured, by measuring the demagnetization of the magnets. This demagnetization was more difficult to measure accurately than the demagnetization of the holding magnets. The reason for that is that the magnetization direction of this magnet is more complicated. It also has smaller size and a shape that is difficult to measure on. Also the measured magnetic field density is extremely sensitive to the distance between the measuring probe and the magnet. The magnets' flux densities before they had been exposed to the MRI scanner were between 40 - 42 mT and afterwards 73 - 90 mT. In order to tell something about the demagnetization of the magnets, a big margin of error has to be accepted. The variance in flux density is kept relatively small and that might also tell more about the demagnetization. If the magnetic flux density afterwards is relatively close to the values before and these values for one distance don't vary much, then the magnets are believed to have been shielded, at least partly . This can then be compared with the results from the unshielded NdFeB holding magnets that were of the same material as the transducer magnets. These magnets lost almost all of their magnetization (91-98.5 %) when they were exposed to the static magnetic field at an angle greater than or equal to 90 degrees during scanning. The transducer magnets that had been exposed to the same conditions, but with soft magnetic material, had high values that were close to each other. Since the values after the exposure was similar to the values before, then soft magnetic material must have shielded the magnets.

5.1.5 Heat generation

The risk of induced temperature because of induced currents has shown to be insignificant compared to other implications on cochlear implants during MRI scanning (Todt et al, 2010). No experimental tests were therefore done on heat generation. For future measurements on heat generation, the test requires the whole BCI system in order to be compared with results from other hearing implants since no heat is generated on the internal holding magnet (Teissl et al, 1998).

5.1.6 Vibrations

The currents induced by the pulsed gradient fields are eddy currents and they occur in metallic conductive object when the exposing magnetic field varies with time. The eddy currents occur according to Lenz law to counteract the gradient field changes in the object by a magnetic field. If this magnetic field is strong enough it will make the object vibrate, which has a potential risk of being unpleasant for the patient (Teissl et al, 1998). In the experiments, vibrations occurred on all magnetic materials that were put inside the scanner and exposed to time-varying fields from image sequences.

The eddy currents will be bigger in the soft magnetic material than in the magnets since the magnets have higher electrical resistivity, see table 5-2.

Material	Electrical resistivity (μΩcm)
Soft magnetic materials	0.35
SmCo	86
NdFeB	160

Table5-2: The electrical resistivity for different magnetic materials. The higher electrical resistivity, the more resistant are the material to induced eddy Currents (Boll, 1979).

5.2 Simulation

5.2.1 Demagnetization

The demagnetization occurs when a torque is induced on the magnet as it is exposed to an applied external magnetic field and the magnet is fixed so it can't align with it. In Figure 4-8 it is possible to see what will happen when the magnet is fixed as it is exposed to this external field. In the top magnet in the image the external field will be cancelled over the magnet and if the external field is greater than the coercive force of that magnet, then it will have been demagnetized when the external field is removed. In the middle magnet in the image no torque will be induced since the magnetization direction is parallel to the external field. If the magnet has a saturation flux greater than its remanence flux density, then this will be reached if the external field is strong enough (Boll, 1979). In the bottom magnet in the image the magnetic fields between the magnet and the scanner are perpendicular; this will induce a torque on the magnet that wants to align all field lines in the same direction. The torque in this case will therefore be directed counter clockwise.

5.2.2 Shielding

In Figure 4-9, the external magnetic field is applied to the transducer as if it was positioned on a patient. In this position, it is possible to see how the magnetic flux density in the transducer is high in the soft magnetic material and therefore lower over the magnets. This keeps the magnets shielded and more difficult to demagnetize.

In Figure 4-10, the external magnetic field is applied to the transducer perpendicular to as if it was positioned on a patient. In this case the shielding doesn't work as good as in Figure 4-9 and the magnets will be exposed to the external magnetic field, experience torque and get demagnetized. The transducer in the simulations is the same as in the experiments and therefore not all parts of it are included. In reality, when the transducer is complete, then it will be shielded for this direction as well, because more soft magnetic material will be used then.

5.2.3 Heat generation

To get an understanding of how the shape of metallic conductive objects in implants will affect the heat generation of that implant, a simulation of a circle and a star is shown in Figure 4-13. The two objects are both electric conductive in a homogenous external electric field. They're surrounded by air and will lead the electric field differently because of their shape. The electric field wants to take the easiest way and since the area at the sharp edges has higher conductivity than the air the field will go that way. This area is very small and the field intensity will therefore be very high there. A high electric field intensity means a high flow of electrical charges through that area. This current flow generates heat when the electric field varies in time (K. Cheng, 1989).

5.2.4 Induced Voltage

No measurements have been made on the induced voltage since it has shown to be insignificant compared to other effects and have not shown to exceed maximum allowed values in other hearing implants. The maximum voltage is limited to not destroy the implant circuitry and is given by the manufacturer. For MED-EL's cochlear implant model Combi4040/Combi40+ this maximum voltage is 6V. The induced signal does not have the same form and amplitude as the signal used for stimulation signals and therefore no undesired signals can be trigged (Teissl et al, 1999). The induced voltage is mostly induced in the receiver coil of the implant. When measuring the induced voltage the maximum signal will be given when the surface of the receiver coil lays in a plane perpendicular to the direction of the transmitted RF-signal, see equation (4). This induced voltage has shown to be strongly dependent on the carrier frequency of the implant receiver coil and not by the magnitude of the static magnetic field of the scanner. The closer the carrier frequency of the receiver coil is to the Larmor frequency, the more voltage will be induced (Teissl et al, 1998). A cochlear implant with carrier frequency of 12MHz gave more induced voltage from a 0.2 T scanner (carrier frequency 8.5MHz) than from a 1.5 T scanner (carrier frequency 63.8 MHz). For the BCI that has a carrier frequency of 120 kHz, the induced voltage will then be high for scanners with lower static magnetic fields, see table 3-1 for the different Larmor frequencies. Since the BCI receiver coil has a carrier frequency much lower than the Larmor frequency of normal scanners, the induced voltage will be more dependent on the peak intensity of the RF-signal (Teissl et al, 1998). For cochlear implants, auditory sensations have been reported for RF-pulses that have been induced in the electrode lead using 1.5T scanners (Hochmair, 2001).

6 Conclusions

The magnets that were used for imaging artifacts for different image sequences were exposed the most to the fields of the scanner. The reason for that is that the same magnets were used for all different sequences. Since those magnets had to be inside the scanner the longest time, they were more likely to get demagnetized. In table 4-1, these magnets are the ones that got demagnetized with 91 (Type A) and 44.2 % (Type B).

When investigating the effects of magnetic resonance imaging on the BCI and other implants, there will always be forces present as long as there is ferromagnetic material in the implant. These forces can be minimized by different methods. The pulling force can be minimized by the use of a MRI scanner without active shielding. It can also be minimized if the size of the internal holding magnet is minimized. The external holding magnet can be bigger to keep the force between the magnets strong enough if the internal holding magnet is made smaller.

The maximum rotational force of the internal holding magnet will be the greatest of all forces and can only be removed if the magnet is allowed to move freely and align with the external field. The maximum rotational force will be the same for all MRI scanners with the same static magnetic field strengths, but the pulling force will depend on the active shielding of the scanner. The ratio between the maximum rotational force and the pulling force will therefore be different for different scanners.

It is possible to measure the force for one magnet and then use that information to calculate the force for another magnet with known magnetic moment. The maximum allowed force of CI's is up to 10N (Vincent et al, 2008).

The idea to have a compression band with a soft magnetic material for fixation of the implant will induce additional forces on the soft magnetic material. This force is relatively small compared to other forces and then there might also be a chance that the soft magnetic material will shield the implant from demagnetization. This will give the magnet an increased magnetic moment.

The image artifacts have shown to be strongly dependent on the choice of image sequence. For SE sequences, a better image was achieved with a higher pixel bandwidth. The smallest image artifact was limited to a circle diameter of 7cm on an NdFeB magnet, see table 4-5. It has also been shown to be possible to use a GE sequence. There will be artifacts with this sequence, but they will be limited as in table 4-6. The artifacts can also be reduced by choosing the phase-encoding direction and frequency-coding direction properly. The magnet can't interfere with the frequency-encoding when their fields are perpendicular (Teissl et al, 1998).

For all the images it is possible to see that the artifacts from the SmCo magnet always are greater than those from the NdFeB magnet. The NdFeB magnet has higher flux density than the SmCo and was therefore expected to distort the image the most, but since it gets demagnetized in the scanner, it looses its magnetic strength which probably is the reason for the smaller artifacts.

The measuring method of the shielding of the transducer magnets is inaccurate, but the magnets are shielded by the soft magnetic material to some extent even if it is difficult to tell exactly how much. The high static magnetic fields of MRI scanners require higher flux saturations of the soft magnetic materials used for shielding.

Objects of materials with higher electrical resistivity are more resistant to eddy currents and are therefore preferable in MRI applications when heat generation is a problem (Shellock et al, 2005). SmCo magnets have lower electrical resistivity than NdFeB magnets, while soft magnetic materials have much lower electrical resistivity than both these magnets.

When scanning another part of the body than the head, the vibrations can be reduced by the use of local RF-coils. Then the transmitted RF pulse only affects the object inside the coil since the signal on the outside will be low.

Newer cochlear implants have been designed to be MRI compatible and been reported to be safe up to 1.5 T for the internal part of the implant without removing the internal holding magnet. MED-EL's C40+ PULSAR and SONATA are CE[1] approved for 0.2 T, 1.0 T and 1.5 T. With removable internal magnets, then some more devices are approved, such as Cochlear TM CI24M, CI24R(CS), Nucleus Freedom and CI24ABI and from Advanced Bionics Corporation HiRes90K (Majdani et al, 2009).

7 References

Boll R (1979) Soft Magnetic Materials, The Vacuumschmelze Handbook: London: Heyden & Son Ltd.

C. Bushong S (2003). Third Edition Magnetic Resonance Imaging: Physical and Biological Principles. Texas: Mosby.

Carlsson Å. Susceptibility effects in MRI and ^{1}H MRS: The spurious echo artifact and susceptibility measurements. Department of Radiation Physics, University of Gothenburg, Sahlgrenska University Hospital, Doctorial Thesis 2009.

Ellis D (2007). [Online] Cell-level 9T MRI. Health Futures Digest, Diagnostics & Imaging http://hfd.dmc.org/articlecomment/?id=8&sid=1#9T [2011-06-04].

Hochmair ES. MRI safety of Med-El C40/C40+ cochlear implants. CochlearImplants International 2001;2:98-114.

Håkansson B, Eeg-Olofsson M, Reinfeldt S, Stenfelt S and Granström G. Percutaneous Versus Transcutaneous Bone Conduction Implant System: A Feasibility Study on a Cadaver Head. Otol Neurotol 2008; 29:1132-1139.

Håkansson B, Reinfeldt S, Taghavi H, Eeg-Olofsson M, Ostli P, Adler J, Gabrielsson J, Stenfelt S and Granström G. A novel bone conduction implant (BCI): Engineering aspects and pre-clinical studies. International Journal of Audiology 2010;49:203-215.

Håkansson B. The balanced electromagnetic separation transducer: A new bone conduction transducer. J. Acoust. Soc. Am 2003;113:818-825.

Jesacher M O, Kiefer J, Zierhofer C and Fauser C. Torque Measurements of the Ossicular Chain: Implication on the MRI Safety of Hearing Implant Vibrant Soundbridge. Otol Neurotol 2010;31:676-680.

K. Cheng D (1989) Field and Wave Electromagnetics (2nd Edition). USA: Prentice Hall.

Majdani O, Leinung M, Rau T, Akbarian A, Zimmerling M, Lenarz M, Lenartz T and Labadie R. Demagnetization of cochlear implants and temperature changes in 3.0 T environment. Otolaryngol Head Neck Surg 2008;138:833-839.

Majdani O, Rau T, Götz F, Zimmerling M, Lenartz M, Lenartz T, Labadie R and Leinung M. Artifacts caused by cochlear implants with non-removable magnets in 3T MRI: phantom and cadaveric studies. Otology 2009;266:1885-1890.

Nordling C and Österman J (2006) Physics Handbook 8th edition: for Science and Engineering: Lund Studentlitteratur.

Shellock FG. Guest Editorial. Comments on MRI heating tests of critical implants. Journal of Magnetic Resonance Imaging. 2007;26:1182-1185.

Shellock FG, Nyenhuis JA, Park SM, Kamondetdacha R, Amjad A, Rezai A. MRI and implanted medical devices: basic interactions with an emphasis on heating. IEEE Transactions on Device and Materials Reliability 2005;5:467-478.

Teissl C, Kremser C, Hochmair E S, Ingeborg J and Hochmair D (1998) Cochlear implants: in vitro investigation of electromagnetic interference at MR imagingcompatibility and safety aspects. Radiology 208:700–708.

Teissl C, Kremser C, Hochmair E S, Ingeborg J and Hochmair D. Magnetic Resonance Imaging and Cochlear Implants: Compatibility and Safety Aspects. J Magn Reson Imaging 1999;9:26-38.

Todt I, Rademacher G, Wagner F, Schedlbauer E, Wagner J, Basta D and Ernst A. Magnetic resonance imaging safety of the floating mass transducer. Otol Neurotol 2010;31:1435-1440.

Vincent C, Ruzza I, Vaneecloo F.M and Dubrulle F. Magnetic Resonance imaging with the Digisonic SP Neurelec cochlear implant. Otology 2008;265:1043-1046.

8 Appendix

8.1 Units

Description	SI Unit
Magnetic moment	Am^2
Magnetic torque	Nm
Permeability of free space	H/m = Vs/Am = Wb/Am= Tm/A
Magnetic flux density	$T = Vs/m^2 = Wb/m^2$
Magnetic field	A/m
Electric field	V/m

Table 8-1. Useful SI-units for calculations on magnetic materials (Boll, 1979).